IDENTIFICATION AND LOCALIZATION ON A WIRELESS MAGNETIC SENSOR NETWORK

A THESIS SUBMITTED TO
THE GRADUATE SCHOOL OF NATURAL AND APPLIED SCIENCES
OF
MIDDLE EAST TECHNICAL UNIVERSITY

BY

SAJJAD BAGHAEE

IN PARTIAL FULFILLMENT OF THE REQUIREMENTS
FOR
THE DEGREE OF MASTER OF SCIENCE
IN
ELECTRICAL AND ELECTRONICS ENGINEERING

JUNE 2012

Approval of the thesis:

IDENTIFICATION AND LOCALIZATION ON A WIRELESS MAGNETIC SENSOR NETWORK

submitted by **SAJJAD BAGHAEE** in partial fulfillment of the requirements for the degree of **Master of Science in Electrical and Electronics Engineering Department, Middle East Technical University** by,

Prof. Dr. Canan Özgen _____
Director, Graduate School of **Natural and Applied Sciences**

Prof. İsmet Erkmen _____
Head of Department, **Electrical and Electronics Engineering**

Assoc. Prof. Dr. Elif Uysal-Bıyıkoğlu _____
Supervisor, **Dept. of Electrical and Electronics Engineering, METU**

Assist. Prof. Dr. Sevgi Zübeyde Gürbüz _____
Co-Supervisor, **Dept. of Electrical and Electronics Engineering, TOBB ETÜ**

Examining Committee Members:

Assoc. Prof. Dr. Ali Özgür Yılmaz _____
Department of Electrical and Electronics Engineering, METU

Assoc. Prof. Dr. Elif Uysal-Bıyıkoğlu _____
Department of Electrical and Electronics Engineering, METU

Assoc. Prof. Dr. Çağatay Candan _____
Department of Electrical and Electronics Engineering, METU

Assist. Prof. Dr. A. Behzat Şahin _____
Department of Electrical and Electronics Engineering, METU

Assist. Prof. Dr. Ali Cafer Gürbüz _____
Department of Electrical and Electronics Engineering, TOBB ETÜ

Date: 12.06.2012

I hereby declare that all information in this document has been obtained and presented in accordance with academic rules and ethical conduct. I also declare that, as required by these rules and conduct, I have fully cited and referenced all material and results that are not original to this work.

Name, Last name: SAJJAD BAGHAEE

Signature :

ABSTRACT

IDENTIFICATION AND LOCALIZATION
ON A WIRELESS MAGNETIC SENSOR NETWORK

Baghaee, Sajjad
M.Sc., Department of Electrical and Electronics Engineering
Supervisor: Assoc. Prof. Dr. Elif Uysal-Bıyıkoğlu
Co-Supervisor: Assist. Prof. Dr. Sevgi Zübeyde Gürbüz

June 2012, 70 pages

This study focused on using magnetic sensors for localization and identification of targets with a wireless sensor network (WSN). A wireless sensor network with MICAz motes was set up utilizing a centralized tree-based system. The MTS310, which is equipped with a 2-axis magnetic sensor was used as the sensor board on MICAz motes. The use of magnetic sensors in wireless sensor networks is a topic that has gained limited attention in comparison to that of other sensors. Research has generally focused on the detection of large ferromagnetic targets (e.g., cars and airplanes). Moreover, the changes in the magnetic field intensity measured by the sensor have been used to obtain simple information, such as target direction or whether or not the target has passed a certain point. This work aims at understanding the sensing limitations of magnetic sensors by considering small-scale targets moving within a 30 cm radius. Four heavy iron bars were used as test targets in this study. Target detection, identification and sequential localization were accomplished using the Minimum Euclidean Distance (MED) method. The results show the accuracy of this method for this job. Different forms of sensor sensing region discretization were considered. Target identification was done on the boundaries of sensing regions. Different gateways were selected as entrance point for identification point and the results of them were

compared with each other. An online ILS system was implemented and continuous movements of the ferromagnetic objects were monitored. The undesirable factors which affect the measurements were discussed and techniques to reduce or eliminate faulty measurements are presented. A magnetic sensor orientation detector and set/reset strap have been designed and fabricated. Orthogonal Matching Pursuit (OMP) algorithm was proposed for multiple sensors multiple target case in ILS systems as a future work. This study can then be used to design energy-efficient, intelligent magnetic sensor networks

Keywords: Wireless Sensor Network, WSN, Magnetic Sensor, Identification, Localization, sequential localization, Minimum Euclidean Distance (MED), Tracking, Orthogonal Matching Pursuit Method, OMP

ÖZ

KABLOSUZ BİR MANYETİK ALGILAYICI AĞINDA
HEDEF TANIMA VE KONUM BELİRLEME

Baghaee, Sajjad
Yuksek Lisans, Elektrik Elektronik Mühendisliği Bölümü
Tez Yöneticisi : Doç. Dr. Elif Uysal Bıyıkoğlu
Ortak Tez Yöneticisi: Yrd .Doç. Dr.Sevgi Zübeyde Gürbüz

Haziran 2012, 70 sayfa

Bu çalışmada, kablosuz algılayıcı ağlarda manyetik algılayıcılar kullanılarak hedef konumlandırma ve tanımlama üzerine odaklanılmıştır. MICAz zerrelerden oluşan ve "Merkezileştirilmiş ağaç-tabanlı" yapıya sahip bir kablosuz algılayıcı ağı kurulmuştur. 2-eksenli manyetik algılayıcı içeren MTS310, MICAz düğümleri üzerinde algılayıcı kart olarak kullanılmıştır. Kablosuz algılayıcı ağlarında (KAA) manyetik algılayıcıların kullanımı, diğer algılayıcı tiplerinin kullanımına kıyasla daha sınırlı olarak incelenmiştir. Araştırmalar genellikle büyük ferromanyetik hedeflerin (araba, uçak, vb.) tespitine yönelik yapılmıştır. Ayrıca, algılayıcılarla manyetik alan yoğunluğunun değişim ölçümleri, hedefin doğrultusu ya da belirli bir noktadan geçip geçmediği gibi basit düzeyde bilgileri elde etmek için kullanılmıştır. Bu çalışmada, 30 cm yarıçap içinde hareket eden küçük ölçekli hedefler için algılama sınırlarının incelenmesi amaçlanmıştır. Çalışma için dört adet ağır demir çubuk, test hedefleri olarak kullanılmıştır. Hedef belirleme, tanımlama ve sıralı konumlama işlemleri Minimum Öklid Uzaklığı metodu kullanılarak yapılmıştır. Test sonuçları, bu metodunun bu işlemler için kullanımının doğruluğunu göstermiştir. Algılayıcı algılama bölgelerinin bölgelere ayrılmasında birbirinden farklı formlar göz önünde bulundurulmuştur. Hedef belirleme, algılayıcıların algılama bölgelerinin sınırlarında yapılmıştır. Çeşitli giriş noktaları belirleme noktası olarak seçilmiş ve sonuçları karşılaştırılmıştır. Canlı bir Belirleme-Konumlandırma-İzleme sistemi kullanılmış

ve ferromanyetik hedeflerin sürekli hareketleri gözlemlenmiştir. Ölçümleri etkileyen istenmeyen etkenler belirlenmiş ve yanlış ölçümleri azaltmak veya ortadan kaldırmak için teknikler sunulmuştur. Manyetik algılayıcıların doğrultusunu bulmak ve set/reset ayarlarını yapmak için birer cihaz oluşturulmuştur. Böylece, bu çalışma sonuçları enerji verimli ve akıllı manyetik algılayıcı ağlarının tasarımında kullanılabilir.

Anahtar Kelimeler: Kablosuz Algılayıcı Ağlarında, KAA, Manyetik Algılayıcı , Tanımlama, Konumlama, sıralı konumlama, Minimum Öklid Uzaklığı metodu, Takip, Dikgen Eşleştirme Metodu, OMP

To my fiancee, mother and father

ACKNOWLEDGMENTS

This dissertation would not have been possible without the support and help of many people. It is a pleasure to convey my gratitude to them all in my humble acknowledgment.

Above all, the useful advice, support and friendship of my supervisor, Prof. Elif Uysal Bıyıkoğlu, has been invaluable on both academic and personal level, for which I am extremely grateful. During the research, when I was encountering with an issue, her encouragements, smiling face and also intellectual guidances have enlighted the dim route of this investigation.

Special thanks are dedicated to my co-supervisor, Prof. Sevgi Zübeyde Gürbüz, because of her wide knowledge, great perseverance and kindness that were so effective during my research. Her constant encouragement has been the motivating factor for this study. I feel very fortunate for having a co-supervisor like Prof. Sevgi Zübeyde Gürbüz, who understood the problems of the research very well and provided effective solutions for them.

Most importantly, my graduation would have not been possible without the love and patience of my family. My parents have been a permanent source of love, concern, support and strength all of the moments in this period. I would like to express my heart-felt gratitude to my fiancee for her patience and love. I would like to dedicate this study to my all family whom I am proud of.

I would also like to thanks my friends Mohammad Maadi, Baran Tan Bacınoğlu, Özlem Derya Erdoğan and Ramin Rezaei for their valuable helps during the experiments.

I take this opportunity to thank Parto Afshan Aria Co., for its technical support in some parts of this reseach.

Finally, I appreciate the financial support from TUBITAK under project 110E252 that funded most parts of the research of this dissertation.

Thank you...

TABLE OF CONTENTS

LIST OF TABLES

TABLES

LIST OF FIGURES

FIGURES

CHAPTER 1

INTRODUCTION

Nowadays distributed wireless sensor networks (WSN) have been widely used for various range of applications such as military, civilian applications in order to monitor the physical and environmental condition like temperature, sound, humid, change of magnetic field of the monitored area, vibration and etc. The main aim of a WSN is detecting, classifying or identifying, localizing and tracking one or more objects in WSN coverage.

For target localization and tracking there are several ways to spread the wireless sensors on the sensing area. We introduce two different class for sensor spreading in monitoring area:

Class one: In some WSN, coverage region of sensors overlap to the extent that every point in the regions is covered by at least one sensor. This kind of sensor spreading guarantees the correctness of the collected data and increases the reliability of the estimations. Energy of the sensors is generally finite and usually rely on the power supplied by battery. The energy consumption and life time of the network is one of the main issues which must be considered as a main point for topology of the spreading the sensors on the monitoring area. This class requires a large number of the sensors in order to cover an area completely.

Class two: In other class of the WSN there are gaps between the sensing areas of the sensors, which we call blind zones. In the blind zones target detection is impossible and the collected data cannot guarantee the reliability of the variations in the monitoring region sufficiently. This is the main disadvantage of the second distributed class.

We applied the sparse network which is optimal form of these two defined classes. The sensors were spread on the area such that they will have minimum sensing region intersection with adjacent sensor sensing region. Under this form of distribution, minimal amount blind zone in monitoring zone for the given number of sensors. By applying this very simple method, minimum number of the sensor can be used for covering an area to compare with class one.

In class two, since fewer sensors are used for covering an area, the cost of this class is less than the cost of the first class. But a system in class one is more reliable than in class two.

In sparse networks, each sensor has its own region. When a target enters to the region of a sensor, that sensor can distribute a message which contains the location of the target. This

message can be used by other sensors to switch their status to sleep mode and save the energy of the battery. By this method we can increase the life time of the network.

In recent years the application of wireless ad-hoc magnetic sensor networks has been widely increased in academic and industrial field for detection, localization and tracking an object. To estimate road traffic patterns and traffic measurement, object detection schemes have been used in [1][2]. WSN is used for aiding the cars in locating parking spaces with intelligent traffic guidance systems in [3][4]. For object classification, magnetic sensors are used in [2][5][6]. In these studies magnetic signatures of the ferromagnetic objects was considered for target identification. Multiple targets tracking, detection and classification on the airport surfaces is discussed in [7].

In all of the reported literature, large ferromagnetic objects, such as cars and airplanes are used as a target for detection, tracking and classification. In this research small objects (metal bars) are used as targets. The accuracy and sensitivity of the sensors are considered in this study. Resolution of the detection and localization of a target is one the main concepts of this research. For achieving this purpose small ferromagnetic targets are selected at related experiments which have small bases. Detection, identification, localization and sequential localization subjects for small targets rather than vehicle or airplane were considered.

In our research team's previous work [8] for estimating the location of a target Least-Squares Estimation was used. This estimator will choose the parameter vector P such that the difference between the magnetic signal model data and measurements is minimized. In [8] for solving the global optimization problems the simulated annealing [9] was used. Unfortunately this method is not useful for multi-target localization and tracking. To incorporate multi-target situation and enable feature extraction, the Minimum Euclidean Distance (MED) method is used in this study and the orthogonal matching pursuit (OMP) is introduced as an extention which may be considered for multiple sensor multiple target (MSMT) cases.

OMP is used in variety of the situation such as Signal Recovery [10][11] radar-based human detection [12] detection and location estimation of metal target under the ground [13].

According to the results of the experiments, we find that the Minimum Euclidean Distance (MED) method could be a good estimator like our previous estimator which we used in [8] for estimating the location of a target.

1.1 Aim of the Study

The purpose of this thesis is to evaluate the use of a Wireless Magnetic Sensor Network in number of fields including target identification, localization and sequential localization. The use of magnetic sensors in wireless sensor networks is a topic that has gained limited attention in comparison to that of other sensors. This study focuses on magnetic sensors while small ferromagnetic objects selected as a target. Sensing limitations of the magnetic sensors are

determined. Extracted additional information can be used in cognitive and adaptive WSN's. Cognitive system can optimize the energy efficiency and performance. In this range of studies, orthogonal matching pursuit (OMP) was proposed as future work for the first time for target identification, localization and tracking by our research team. An online demonstration code was generated for displaying a target movement.

1.2 Abbreviations

In this study a wireless sensor network will be abbreviated as by "WSN". MED is shows Minimum Euclidean Distance. "OMP" expresses a greedy algorithm which is short form of the "Orthogonal Matching Pursuit". Each entry of the MED and OMP dictionary is named "atom".

A sensor nodes in WSN which collects the data and process them and communicates with base station on other nodes is called "mote". A MIB520 USB interface board which connected to a laptop is named base station.

The whole of the magnetic sensors, base station, MED and OMP construct a wireless sensor network which was used to target identification, localization and tracking. The name "ILS system" is devoted to this system. ILS system is short form for identification, localization and sequential localization system.

1.3 Scope of the Thesis

This thesis is composed of five main chapters. Brief contents are given below:

Chapter 1: Introduction of the thesis. The objectives and outlines of the study is given in this chapter. The previous works which so similar to this study are expressed.

Chapter 2: Software and hardware which applied for this study is introduced in details.

Chapter 3: Dipole model, Minimum Euclidean Distance (MED) method used in the study.

Chapter 4: Usage of Minimum Euclidean Distance (MED) method for localization and classification of a target in WSN is shown in this chapter. Experimented results are discussed.

Chapter 5: A brief summary, conclusions and future work.

CHAPTER 2

HARDWARE AND SOFTWARE SYSTEM ARCHITECTURE

2.1 Overview

ILS system can be considered in three phases:

- Distributed magnetic sensor senses and obtains the change of the magnetic field. After getting the needed data, the sensor transmits them to the base-station.
- The base-station receives the data from the sensors and does some operation on coming messages.
- Software and Minimum Euclidean Distance (MED) method which operates on the computer for message analyzing, demonstrates any changes in the sensors sensing region or entirely in the network zone.

Since the features of the hardware, software and the algorithm of the ILS system completely affect the processes of the ILS; following chapter has been allocated to explain them in detail.

2.2 The Typical Architecture of a Sensor Node for WSN

A node or mote is the main part of a wireless sensor network which plays the main rule in data collection from its sensing region. After analyzing the data using node's processors, the communication module of the nodes transmits the required data to the base-station or other motes in its domain. A sensor node consists of four main elements:

- Processor unit
- Communication unit (transmitter and receiver)
- Sensing unit like magnetic sensor, light sensor, temperature sensor and etc.
- Power unit

A general architecture of a sensor node is shown in Figure 2.1.

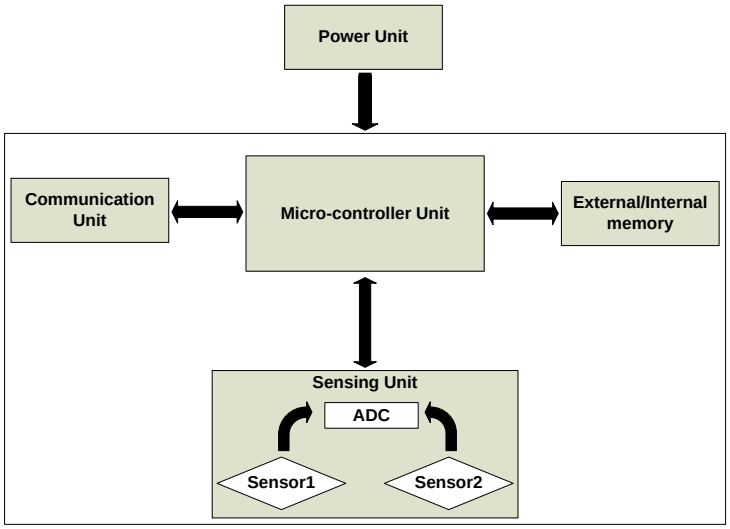

Figure 2.1 The typical architecture of a sensor node for WSN

2.3 Mote

For this study we used MICAz motes and a wireless sensing network was designed with these units. The block diagram of the MICAz [14] is shown in Figure 2.2.

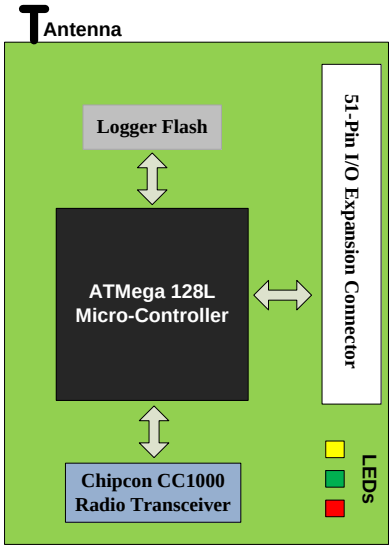

Figure 2.2 Up view of the MPR2400 / MICAz mote [14]

Among mote products of Crossbow Technology, the MICAz is the final provided one. MICAz microcontroller is based on an ATMEGA 128L. This microcontroller has a 128 Kbytes Flash program memory and a 4 Kbytes SRAM [15]. These kinds of motes also have Chipcon CC2420 transceiver as RF Module and IEEE 802.15.4 compliant. The radio operates in the 2.4 GHz unlicensed ISM band. Under worldwide regulation surveillances, it covered by ETSI EN 300 328 and EN 300 440 class 2 (Europe), FCC CFR47 Part 15 (US) and ARIB STD-T66 (Japan). Digital direct sequence spread spectrum baseband modem which is in CC2420, provides a spreading gain of 9 dB and an effective data rate of 250 kbps [16].

Two AA type batteries provide the sensor supply voltage. In fact, any batteries with power supply in the range of 2.7 to 3.6 VDC can be acceptable although the power supply should not be reduced below 2.7 VDC [14].

2.4 Sensor Board

MICAz are equipped with MTS310CB sensor board [17]. This sensor board is shown in Figure 2.3.

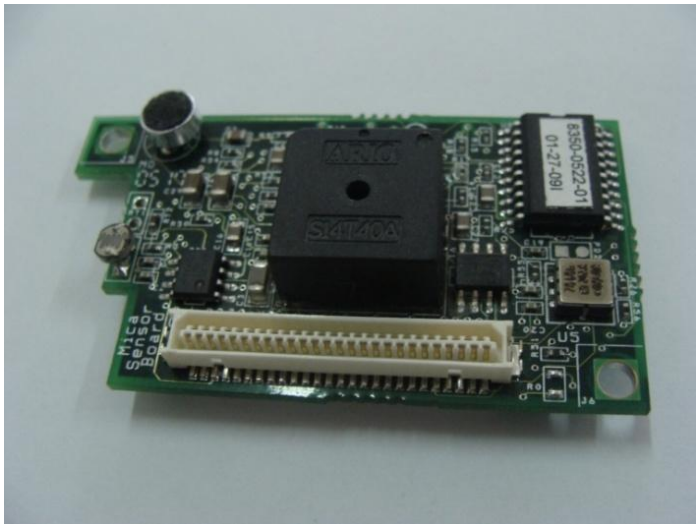

Figure 2.3 MTS310CB sensor board

Different kinds of sensors are fabricated on MTS310CB sensor board and make it so flexible for wide range of sensing applications such as monitoring the environment temperature with Panasonic ERT-J1VR103J thermistor, sensing the changes of the network region magnetic fields

using Honeywell HMC1002 2-axis magnetometer, recording the variation of the light and sounds in the sensing zone with CdSe photocell and a basic circuit with a pre-amplifier and a digital-pot control for amplifying the second stage, respectively and also for movement, vibration and seismic sensing with ADXL202JE 3.4 2-Axis Accelerometer[17]. Among this wide range of sensing instruments for this study we used Honeywell HMC1002 sensor magnetometer (Figure 2.4).

Figure 2.4 Honeywell HMC1002 2-axis magnetometer

According to our observations during the test the capability of detecting a ferromagnetic object with this sensor is closely related with the sensitivity of the sensor and magnetic property of the ferromagnetic object. This topic will be expanded in detail in chapter 2.6.2.

MTS310CD sensor board has a 51-pin expansion connector from bottom for MICAz mote and from top for external boards (Figure 2.5).

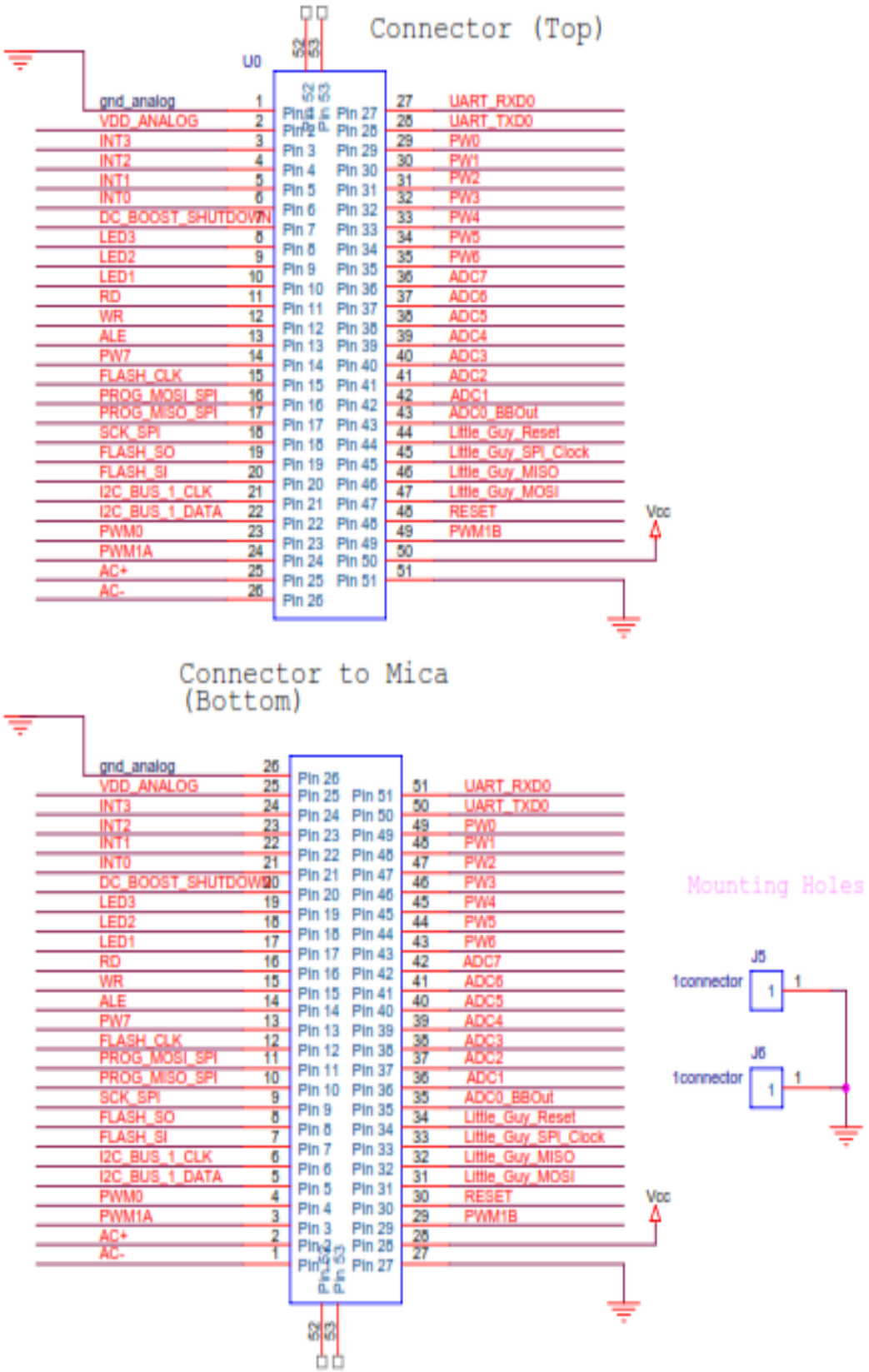

Figure 2.5 Schematic of 51-pin connector pin-outs of MTS310CD sensor board [14]

2.5 MIB520 USB Interface Board

For our investigation we used MIB520CB via 51 pin (male connector) interface board. This board is connected to MICAz mote (Figure 2.6). This device forwards the message to a laptop which is acting as a fusion center via USB port. MIB520 is used to program the MICAz via an on-board in-system processor (ISP) (an Atmega16L). Using laptop USB port, we inject the codes to ISP and afterwards connected mote is programed by ISP [14].

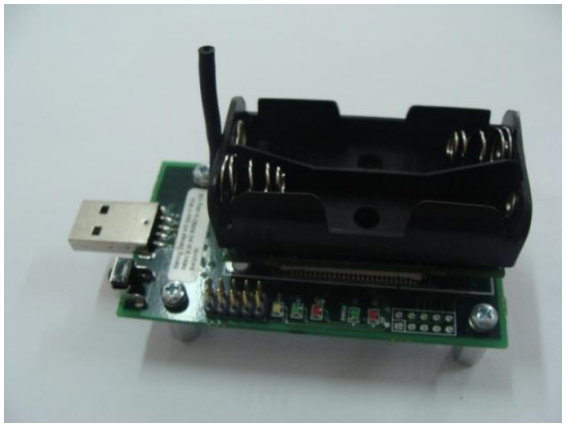

Figure 2.6 MIB520 + MICAz with USB gateway

Power of both MIB520 and the connected mote are supplied through USD bus of the PC. The MIB520CB board is shown in Figure 2.7 [14].

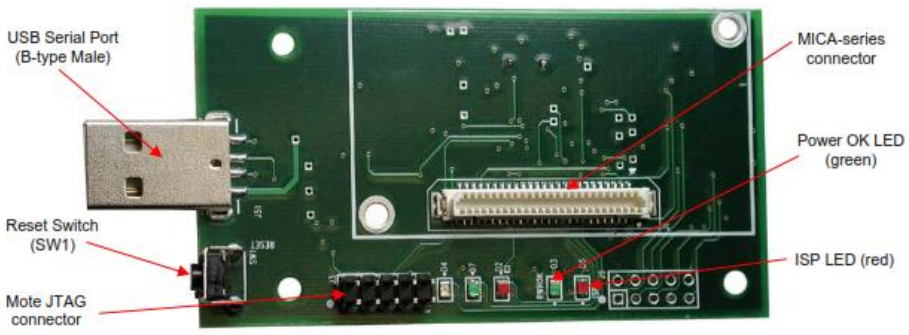

Figure 2.7 The MIB520CB board [14]

2.6 Magnetometer

For this study magnetometer plays an important rule for detecting a ferromagnetic target such as a vehicle and then localizing that object and tracking the target on the sensing region of the network. For detecting the movement of vehicle, the sensor output is typically sampled at 100 Hz. The MTS310 sensor board is equipped with HMC1002 anisotropic magnetoresistive (AMR) magnetic sensor. HMC1002 is a 2-axis magnetic sensor. In each direction (X and Y) of this sensor, there is a Wheatstone bridge which converts the change of the magnetic field to voltage. It measures the ambient or existing magnetic field in each axis when a required voltage (5 V typically) is connected to Wheatstone bridge (V_b).

2.6.1 Operation

Electrical resistance of some materials can be altered when they are exposed by a magnetic field [18]. Magnetoresistive of ferromagnetic metals were discovered by William Thompson and later by Lord Kelvin [19]. This property is applied for creating a new generation of the sensors. These types of sensors are called anisotropic magnetoresistance sensors (AMR sensors). The value and the orientation of the magnetic field can be sensed by these sensors. Nickel-Iron [20] (Permalloy) thin films are used for creating resistive elements of AMR sensors. According to [20], the resistance of the thin film is changed by 2-3%, when an AMR sensor feels magnetic field. For sensing magnetic field four magnetorestive are connected as a "Wheatstone bridge" (Figure 2.8).

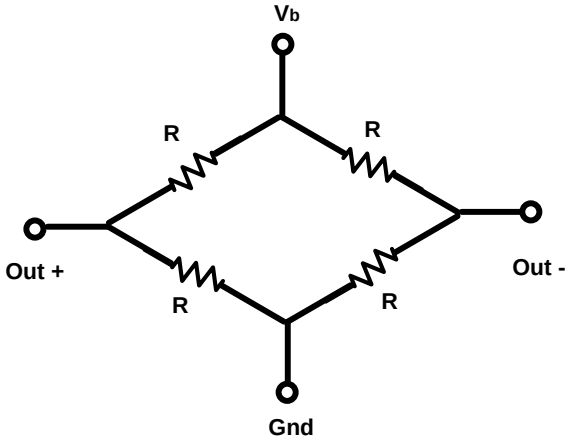

Figure 2.8 Wheatstone bridge - voltage difference between OUT+ and OUT- is measured

When a magnetic field is applied in AMR sensors, the resistance of the two magnetorestive materials will be increased and other two will be decreased. Any magnetic changes make different voltages on the output terminals (OUT+ and OUT-). This value is strongly dependent to the sensor sensitivity, the bridge supply voltage, bridge offset voltage and the applied field [21][8]. Hence the following equation will be obtained:

$$V_{diff} = S \times V_b \times B_s + V_{offset} \quad (2.1)$$

where:

- S is the sensitivity (mV/V_{ex}/Gauss)
- $V_b$is the bridge offset voltage (V)
- B_s is the magnetic flux
- V_{offset} is the bridge offset voltage (mV)

2.6.2 Sensitivity of HMC1002

According to the data sheet of the HMC1002 when 3A current is passed from set/reset, the maximum, minimum and typical value for sensitivity will be 4, 2.5 and 3.2 respectively [22]. To calibrate other sensors, we should select one sensor as a reference sensor and the sensitivity of that sensor should be 3.2. To do this, we should select a location with name of "C" for sensors where there is a target in distance R (point "T") from point "C" (Figure 2.9). At first step the reference sensor is put at point "C" and the equation 2.2 [8] is used for obtaining the magnetic intensity of that target and sensing zone (B_{Target}) on the sensor.

$$B_{Target} = \frac{ADC_{Target} + 54 \times POT_{Target}}{0.001 \times G_{total} \times ADC_{fullscal} \times 3.2} \quad (2.2)$$

where:

- ADC_{Target} is analog to digital convertor value which we read it from coming messages from sensors.
- POT_{Target} PotentiometerBias value which we read it from coming messages from sensor.
- $ADC_{fullscal} = 2^{10} - 1 = 1023$ (2.3)
- $G_{total} = G_1 \times G_2$ (2.4)

$$G_1 = 5 + \frac{80\ KOhm}{R_{G_1}} \quad (2.5)$$

$$G_2 = 5 + \frac{80\ KOhm}{R_{G_2}} \quad (2.6)$$

R_{G_1} and R_{G_2} are external resistors on the magnetometer circuit for adjusting the gain of each amplifier.

In second step we should place other sensors one by one at point "C" when the target is remained at point "T". Suppose that the ambient is not changed during the tests. Since we know the B_{Target} the sensitivity of each sensor for each direction can be obtained from the equation 2.7.

$$S = \frac{ADC_{target}+54\times POT_{target}}{0.001 \times G_{total}\times ADC_{fullscal} \times B_{Target}} \quad (2.7)$$

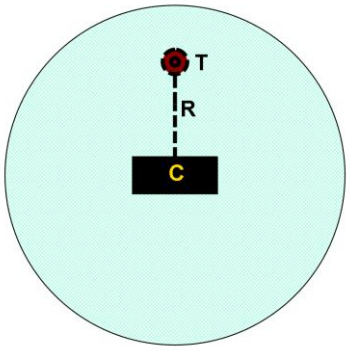

Figure 2.9 Calibrating the sensors

If the accurate value for sensitivity is required two different methods for HMC1002 sensitivity value estimation can be proposed:

Using MilligaussMeter : According to the Figure 2.10.a one MilligaussMeter is located at point A. MilligaussMeter measures the magnetic field while there is no target around that (Ambient value) (B_{am}). After ambient magnetic field measurement, one target is located at point B and then the magnetic field B_{total} measurement is accomplished (Figure 2.10.b). The difference of these two values which is called target actual magnetic field gives us the magnetic effect of target from point B to point A which is shown by B_{target} as following equation:

$$B_{target} = B_{total} - B_{am} \quad (2.8)$$

Next, we locate a sensor at point A while there is no target in sensing region of that target. After reading the ADC (ADC_{am}) and the PotentiometerBias (POT_{am}) values from sensor, the target is located at point B and the reading process of ADC (ADC_{Total}) and PotentiometerBias values (POT_{total}) should be done again. The difference of these two ADC values is shown by

$$ADC_{target}=ADC_{total}-ADC_{am} \quad (2.9)$$

$$POT_{target}=POT_{total}-POT_{am} \quad (2.10)$$

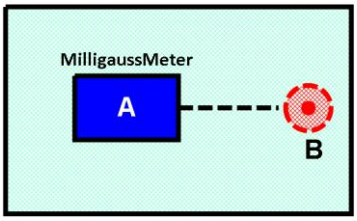

Figure 2.10.a No target around the MilligaussMeter

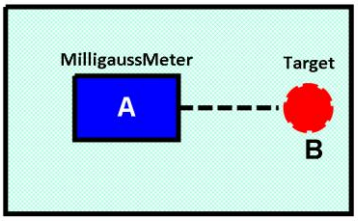

Figure 2.10.b A specific target located at point B

Obtained values should be placed in equation 2.7 [8] for calculating the sensitivity "S" for each sensor at each axis. In Figure 2.11 a MilligaussMeter is shown [23].

Using Helmholtz coil: The earth magnetic field intensity is around 50,000 nT. This field has undesirable effects on measurements of the sensors. In order to reduce this effect (making it zero) and create a known magnetic field with known direction for this field, we can use a Helmholtz coil (Figure 2.12) [24]. The sensor is placed in the Helmholtz coil. After eliminating the effect of the earth magnetic field and generating a known magnetic field by Helmholtz coil, the ADC and PotentiometerBias sensor values can be achieved. The equation 2.5 can be utilized to estimate the sensitivity (S) of that sensor.

Figure 2.11 MilligaussMeter [23]

Figure 2.12 Sensor sensitivity estimating by Helmholtz coil [24]

As mentioned, using two methods we can estimate the sensitivity of the sensors for each direction. Some factors like temperature variation, instruments noises, human fault factors and etc may affect the estimation of the sensitivity. In order to reduce these destructive effects, the measurements must be repeated several times. For having an accurate value for sensitivity estimation, the average of the estimation should be calculated. For example for sensitivity of X axis we have:

$$S_x = \frac{\sum_{i=1}^{N} S_{x_1}}{N} \tag{2.11}$$

where N indicates the number of the estimations

2.6.3 Set/Reset and Offset Straps

As we mentioned in part 2.6, resistive elements of anisotropic magnetoresistance sensors are a combination of Nickel-Iron (Permalloy) thin films. Magnetic domains of AMR sensors have smooth direction. When these domains exposed by high magnetic field (more than 10 gauss), their direction may be eliminated. This elimination crashes their alignment of the magnetization vector. Under this undesirable condition, the sensitivity of the sensors will be decreased and the measurements will not be accurate. For recovering the orientation of the domains and rotating them back to their previous direction, an on-chip coil is placed on Honeywell sensor. For realigning the total magnetization vector with the easy axis, high current pulse is transmitted through the coil. This current generates a strong magnetic field and hence, the domains are realigned again. Ultimately, in order to recovering accurate measurement of the sensors, having a Set/Reset (S/R) strap is essential for AMR sensors. The effect of Set/Reset is shown in Figure 2.13.

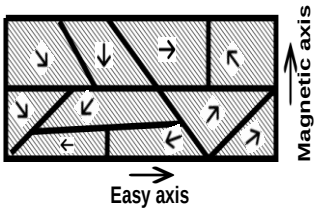

Figure 2.13.a Magnetic domains directions before set/reset pulse

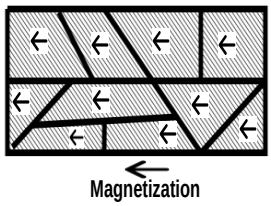

Figure 2.13.b Magnetic domains directions after set/reset pulse R to L

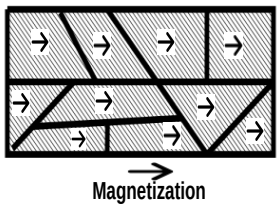

Figure 2.13.c Magnetic domains directions after set/reset pulse L to R

The Set/Reset circuit were designed and fabricated in our laboratory. (Figure 2.14) the current pulse shape and its circuit are shown in Figure 2.15 and 2.16, respectively.

Figure 2.14 Set/Reset device

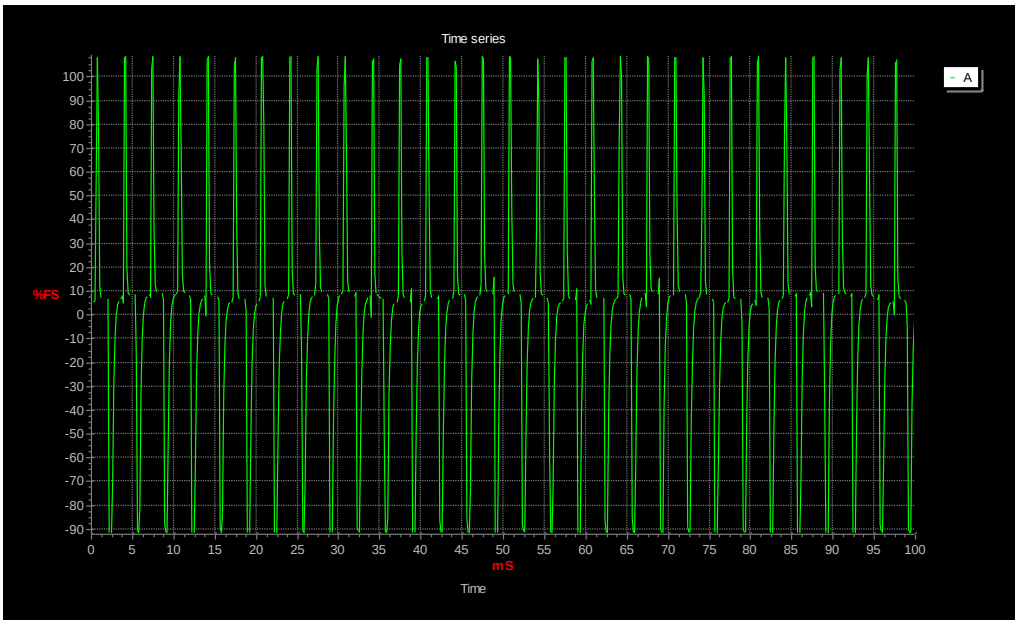

Figure 2.15 Pulse shape which generates by Set/Reset device

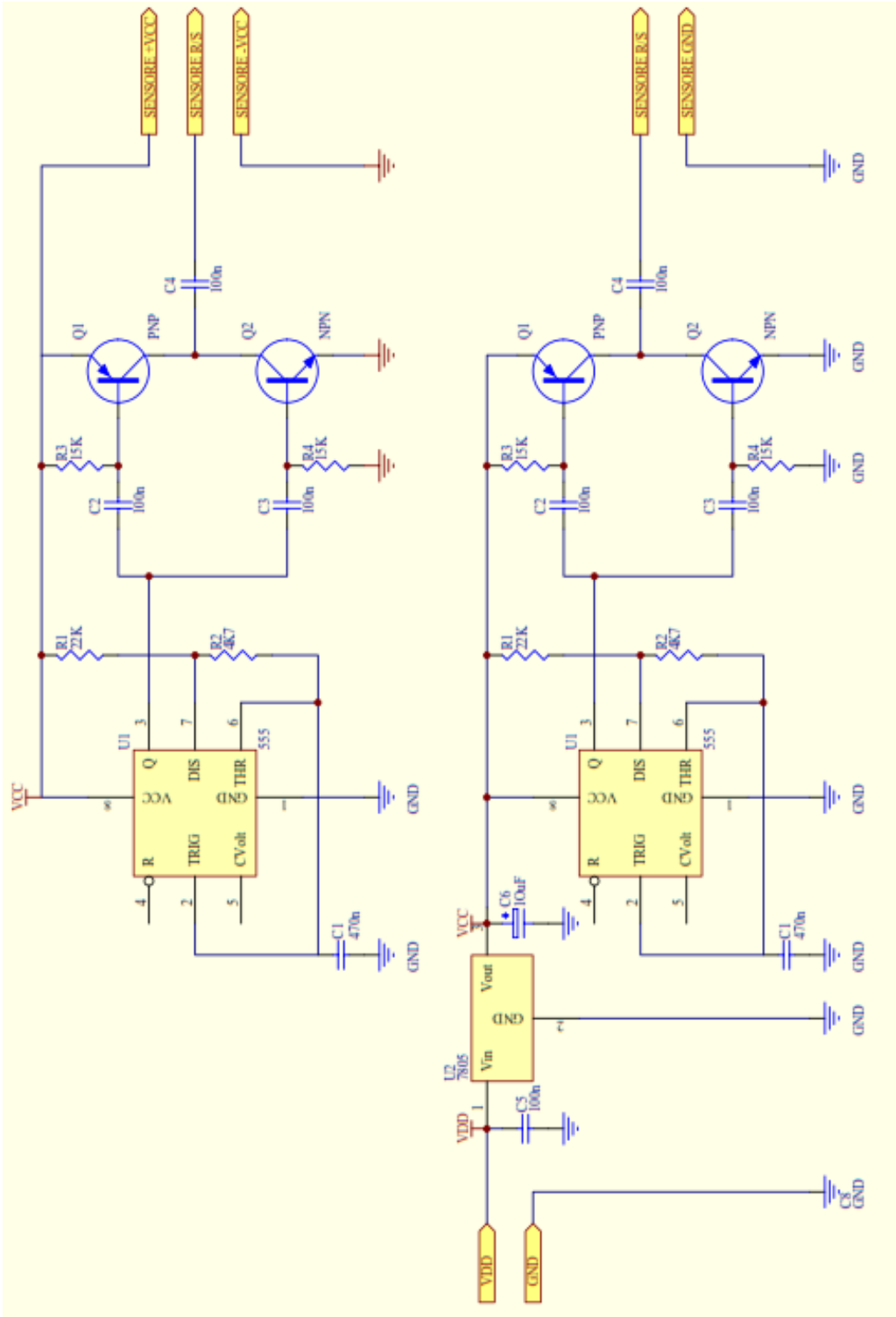

Figure 2.16 Circuit of the Set/Reset device

2.6.4 Magnetic Sensor Axis Orientation

Honeywell HMC1002 is 2-axis sensor (Figure 2.17) [22]. A series of tests presented detecting of a car at a 15 feet radius from the sensor [17]. According to the MTS310CB datasheet (Figure 2.18), ADC5 and ADC6 pins are connected to DieA and DieB on the HMC1002 magnetometer, respectively (Figure 2.17). These directions are selected as a standard axis for HMC1002.

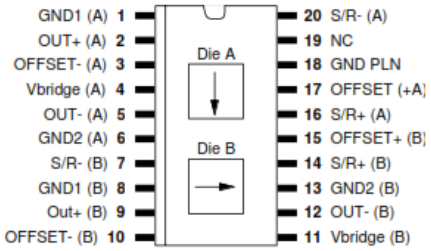

Figure 2.17 Package / pinout specifications of HMC1002 — two-axis AMR microcircuit [22]

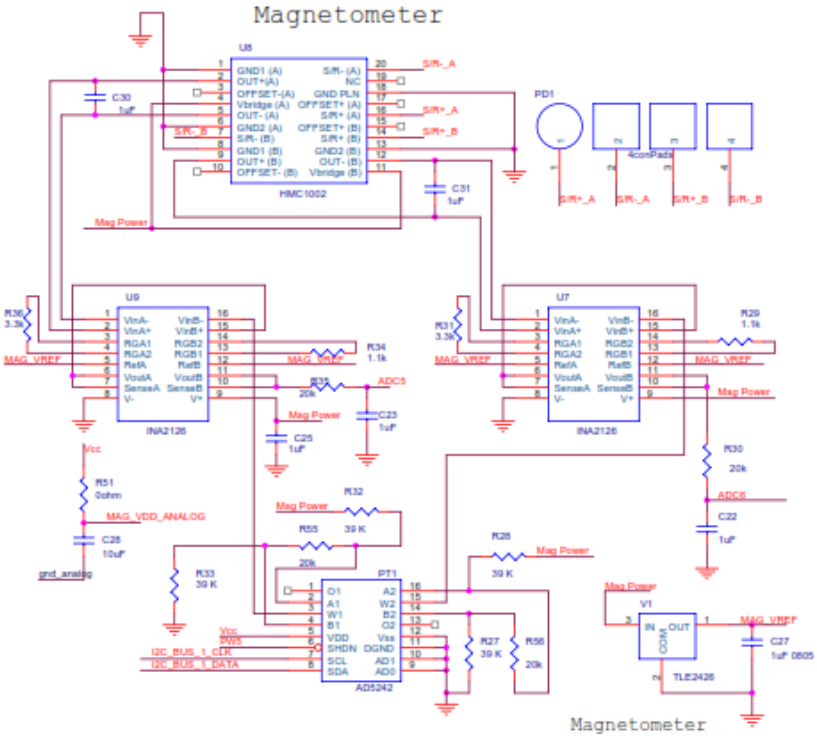

Figure 2.18 MTS310CB magnetometer circuit diagram [17]

During the experiments, for different sensors we found different sensor axis directions in the laboratory. With two different methods, we clarified the axis orientation for each sensor.

2.6.4.1 Comparing the Magnetic Field Curve Changes With a Theoretical Curve

Since we know that, the magnetic field of the sensor will be changed, if a ferromagnetic object gets close to it and by considering the standard axis directions(Figure 2.17), all of the possible magnetic field curves are plotted (Figure 2.19).

For detecting the direction of the sensors, we used an oscilloscope. The magnetic field variations were monitored while a ferromagnetic target was moved in front or behind sides of the sensors. The observed plots in the oscilloscope were compared with the shown ones by Figure 2.19.

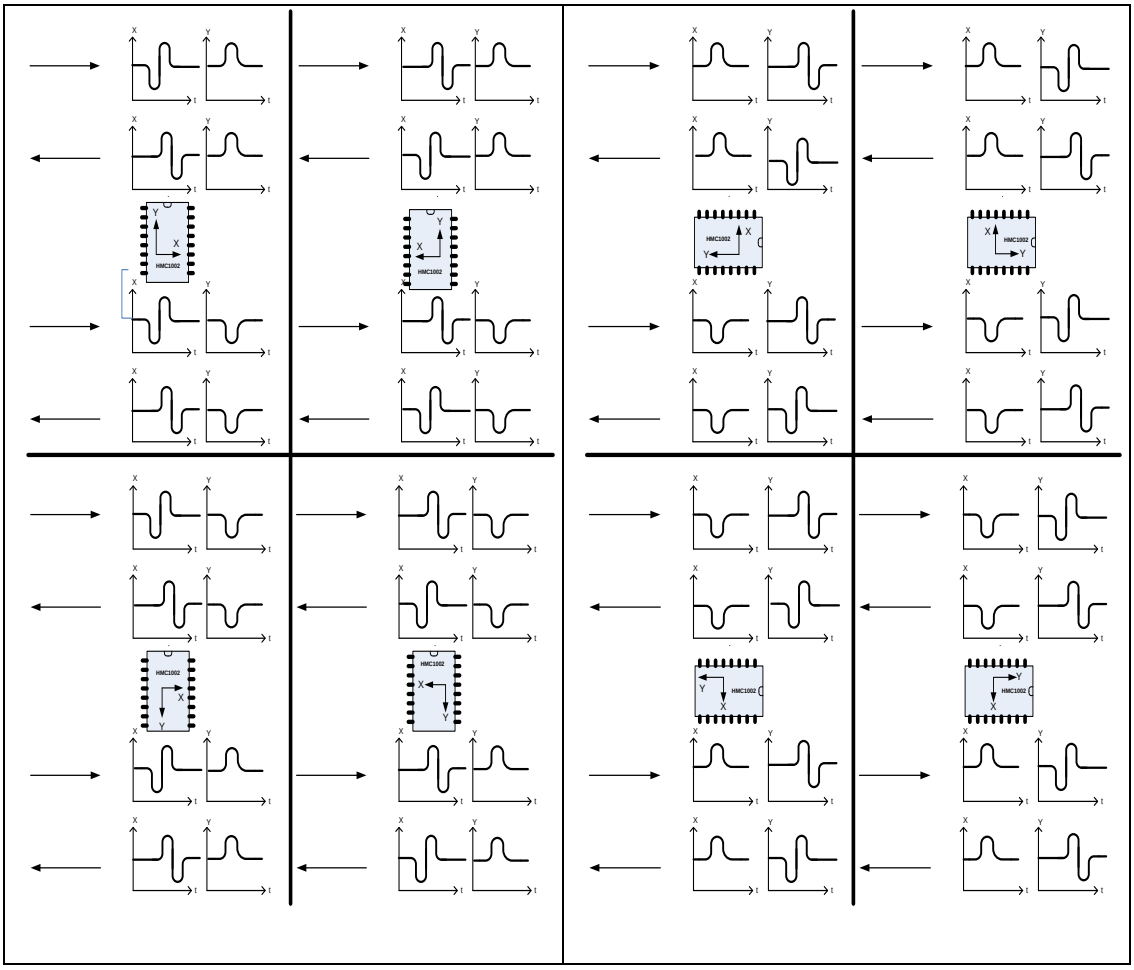

Figure 2.19 Theoretical curves for magnetic field changes

2.6.4.2 Sensor Axis Orientation Detector Instrument

We designed and fabricated an instrument to detect the axis orientation of the sensors (Figure 2.20).

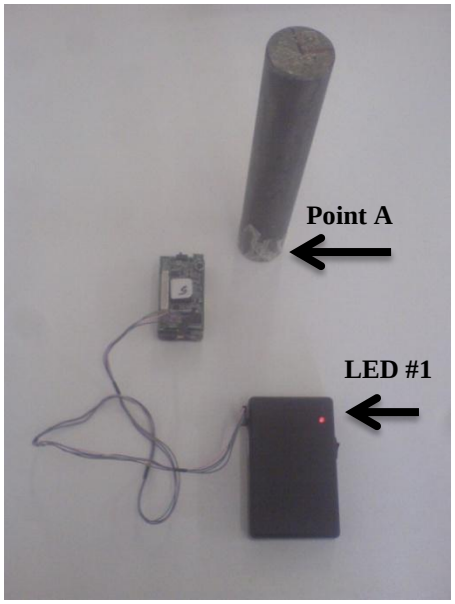

Figure 2.20.a Axis orientation detector. LED #1 is on when a target located at point A

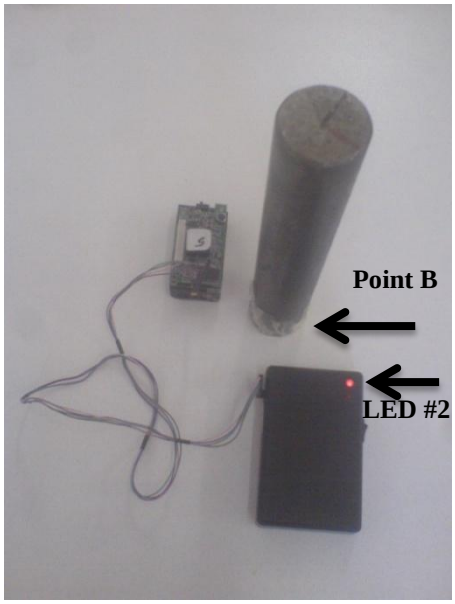

Figure 2.20.b Axis orientation detector. LED #1 is on when a target located at point B

When a target is in the sensing region of the HMC1002 in distance of R from the sensor, an electrical potential deference is generated between pins 2 and 5 of HMC1002 for axis DieA and pins 9 and 12 for axis DieB (Figure 2.17). The values of these voltages are used in this method for detecting the orientation of the axis. We used a LM324, two resistances (R_f and R_1) and two LEDs. The layout of this axis direction detector is shown in Figure 2.21.

When a test target was located at distance of 10 cm from the X axis (or Y axis) of the sensor, the voltage between pin 2 [+A] and pin 5[-A] (pin 9 [+B] and pin 12[-B]) was 0.011 volt. This value was selected as V_{in} for Sensor Axis Orientation detector instrument. This device is a kind of a Non-inverter Amplifier. The equation 2.12 is valid for this circuit.

$$\frac{V_{out}}{V_{in}} = 1 + \left(\frac{R_f}{R_1}\right) \tag{2.12}$$

By previous experiments R_f was chosen 47000 Ω (Large resistance). The V_{in} is 0.011 volt for this circuit. Since the value "1" in comparison with R_f/R_1 is negligible then it can be ignored from the equation 2.12, so we will have:

$$\frac{V_{out}}{0.011} = \left(\frac{47000}{R_1}\right) \tag{2.13}$$

To obtain the intended value of the V_{out} for turning LEDs on, we should replace R_1 with different resistance values. Since we know that the value of the V_{out} is around 1.5 V, the R_1 appropriate value can be finalized. With respect to previous clarification and our practical tests, 3.9 kΩ was found for R_1.

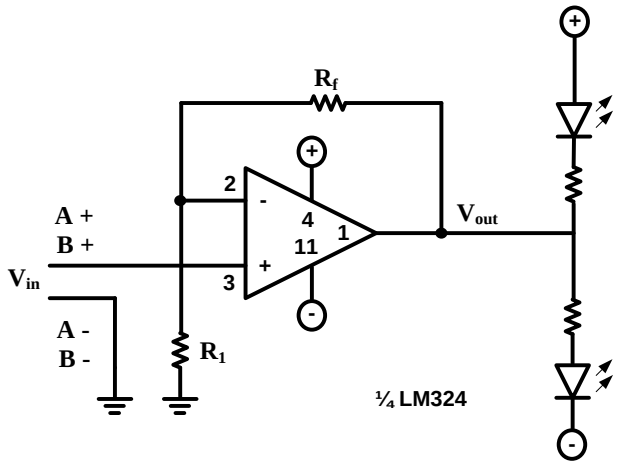

Figure 2.21 The layout of axis orientation detector (non-invert amplifier)

When the located ferromagnetic object is placed at point A the LED number 1 is on and the LED number 2 is off and when this object comes to point B the LED number 1 is off and the LED number 2 is on, inversely. If the LED number 1 is turned on before LED number 2, it means that the Sensor Axis Orientation is parallel to the movement of the ferromagnetic object from A to B (Figure 2.20) but if the LED number 2 is turned on before LED number 1, the Sensor Axis Orientation is parallel to the movement of the ferromagnetic object from B to A. The circuit of the Sensor Axis Orientation detector is designed based on the standard directions. These standard directions have been proposed in HMC1002 datasheet (Figure 2.17).

2.7 Software

There are various kinds of Operating systems (OS) that may be used in some nodes. The popular OS is TinyOS which is based on an event-driven programming model. This operating system is an open source program which uses Network Embedded system-C (NesC)

programming language. The syntax of this language is a modified version of C programming language.

Operating system on the PC was Ubuntu 9.10 and TinyOs 2.1.0 was installed and applied for MICAz mots programing in our Wireless sensors network. For generating and modifying the codes, Eclipse IDE v3.5.0 which is equipped with Yeti2 plugin (a TinyOS plugin) was used.

Processing of the coming data from the network for minimum distance method, demonstrating of the target location and tracking part of the research have been done by MATLAB.

CHAPTER 3

THEORETICAL MODEL AND ALGORITHM

3.1 Overview

Modeling the magnetic field intensity and its variations plays an essential role in this study. Any ferromagnetic object induces a change in the magnetic field intensity in its surroundings. This field has a close relationship with magnetic properties of that ferromagnetic object. Our earth has a uniform magnetic field. The combination of these two magnetic fields provides a new magnetic field which is vital for our measurements. This chapter is devoted to a detailed discussion of these effects and the dipole model to be used for ferromagnetic materials will be introduced.

3.2 The Earth and Magnetic Field

According to the material which presented at [25] the polarity of Earth's magnetic field cannot reverse sharply. According to this report the earth's field may destroyed about 5-15% in 150 years. By this clarification we can assume Earth has a uniform filed distribution over a wide area on the scale of kilometers. In the time scale of the experiments the magnetic field is assumed to be stationary. Magnitude and direction of this field depend on geographic coordinates of the location where the experiment takes place. During the experimentation phase, unexpected variations in magnetic ambient value were observed even under fixed environment conditions for long periods of time. For inspecting these variations a series of experiments has been conducted. The results of these experiments are shown in chapter 4. If the test duration is long or environment conditions change rapidly, the ambient value can change unpredictably. For this reason the presumed ambient value for our ILS system must be updated by considering these variations for having accurate estimation. Our measurements and tests are done in METU (Middle East Technical University), Ankara, and Turkey[1] during the years 2011-2012.

1 According to Google Earth, METU is located approximately at is 39.8914° N, 32.7847° E [26].

3.3 Ferromagnetic Object and Magnetic Field of the Earth

As expressed earth has a uniform filed distribution over a wide area on the scale of kilometers. When a magnetic object enters to a region, the existence of that magnetic object disturbs the uniform magnetic field of the earth at that region. These magnetic field variations are necessary for AMR sensor for sensing the existence of a ferromagnetic object. In Figure 3.1 effect of ferromagnetic object on uniform magnetic field of Earth is shown.

Figure 3.1 Earth's magnetic field and effect of Ferrous object on it

When the electric charge densities are constant and the currents are steady we can use magnetostatic equations. Under this condition the electric and magnetic fields are static [27]. Since we change the position of the target slowly (5 cm/s) in our testbed, the magnetic field also changes slowly. Hence this slowly moving target can be simulated by the magnetostatic equations. As seen in Figure 3.1, combination of the uniform magnetic field of the earth and the disturbance magnetic field of ferromagnetic object, generates a new magnetic field at that region.

A magnetic dipole moment model was used for modeling this disturbance [28] as follows:

$$B(r) = \frac{\mu_0}{4\pi}\frac{1}{r^3}\left[3(\boldsymbol{m}\,.\,\hat{\boldsymbol{r}})\hat{\boldsymbol{r}} - \boldsymbol{m}\right] = \frac{\mu_0}{4\pi}\left[\frac{3(\boldsymbol{m}.\boldsymbol{r})\boldsymbol{r}}{r^5} - \frac{\boldsymbol{m}}{r^3}\right] \quad (3.1)$$

where:

- $\mu_0 = 4\pi \times 10^{-7}$ [T•m/A] is the permeability of vacuum.
- r is L-2 norm of the vector r̂.
- r̂ is the unit vector in r direction
- m is magnetic moment

This equation shows the magnetic field (B) of a point dipole moment m at distance r from ferromagnetic object.

In Cartesian coordinate form of equation (3.1) in x, y and z directions are as follows:

$$B_x(x,y,z) = \frac{\mu_0}{4\pi}\left[\frac{3(m_x x + m_y y + m_z z)x}{[x^2+y^2+z^2]^{\frac{5}{2}}} - \frac{m_x}{[x^2+y^2+z^2]^{\frac{3}{2}}}\right] \quad (3.2)$$

$$B_y(x,y,z) = \frac{\mu_0}{4\pi}\left[\frac{3(m_x x + m_y y + m_z z)y}{[x^2+y^2+z^2]^{\frac{5}{2}}} - \frac{m_y}{[x^2+y^2+z^2]^{\frac{3}{2}}}\right] \quad (3.3)$$

$$B_z(x,y,z) = \frac{\mu_0}{4\pi}\left[\frac{3(m_x x + m_y y + m_z z)z}{[x^2+y^2+z^2]^{\frac{5}{2}}} - \frac{m_z}{[x^2+y^2+z^2]^{\frac{3}{2}}}\right] \quad (3.4)$$

3.4 Targets

For this study in area of the laboratory 5 different iron bars are used as targets (Figure 3.4a and 3.4b). The Alloy which used for producing target number 1, 2, 3 and 4 are Homogeneous. The shape of each target is different but symmetric (Figure 3.1 (a)). Target 5 is combination of the targets number 1 and target number 4, so target number 5 is a non- Homogeneous and non-symmetric target (Figure 3.1 (b)).

For outdoor test we used a car as targets for identification, localization and sequential localization problems (Figure 3.1 (c)).

Target number 5 and cars are composed of different ferromagnetic materials; the disturbance of these composite targets can be modeled as a dipole moment.

Figure 3.1.a Indoor targets, target number 1, 2, 3, 4

Figure 3.1.b Indoor targets, target number 5

Figure 3.1.c Outdoor target

3.5 Minimum Euclidean Distance (MED) Method

According to the clarifications of the section 2.6 each HMC1002 magnetometer has two magnetic sensors in two orthogonal axis (X and Y). In each measurement two values can be observed. One of the values belongs to X axis sensor and other to Y axis sensor. These two values can be represented by a vector in a Cartesian coordinate system.

If two points S and V are represented by their position vectors **S**= $\overrightarrow{OS}$ and **V**= $\overrightarrow{OV}$ respectively, the distance between S and V can be shown by SV. This distance is magnitude of the vector $\overrightarrow{SV}$.

$$\overrightarrow{SV} = \boldsymbol{v} - \boldsymbol{s} \tag{3.5}$$

$$d(S,V) = \mathrm{SV} = |\overrightarrow{SV}| = |\boldsymbol{v} - \boldsymbol{s}| \tag{3.6}$$

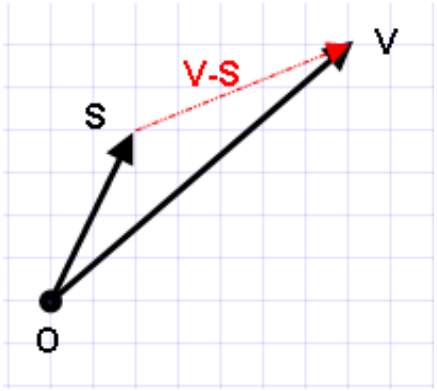

Figure 3.2 Distance between point S and V

Minimum Euclidean Distance (MED) method tries to find a vector among the vectors of a dictionary D which has the maximum similarity with test signal "s". The column of dictionary "D" having maximum correlation with test signal "s" is selected.

In order to use MED method we need a dictionary which is created by using signal parametric model. In our testbed we divided the sensing region of each sensor to 28 sub-regions and 4 sub-regions and obtain data from each point for generating a dictionary. We will discuss about this procedure in greater detail in the next chapter .each element of the dictionary "D" is named atom.

To investigating the similarity of test signal "s" and vectors of the dictionary "D", the distance between the end point of test signal "s" and each vector is considered. Absolut value of the distance of the i^{th} vector form test signal "s" is recorded in i^{th} row of the coefficient vector "C" where the "i" shows the vector number. Among the rows of the coefficient vector "C" which

have the minimum value, will be selected. The rows number of the minumum value shows the similar vector with test signal "s".

MED method:

Input:

- A d-dimensional target signal s and matrix D.

Output:

- A coefficient vector c

1.	$\Lambda_0 = \emptyset$	{ Initialize the index set }
2.	**for** t=1 to I **do**	{ I=Dimension of the Dictionary D}
3.	$d_t(s,v) = \sqrt{\sum_{k=1}^{d}(v_k - s_v)^2}$	{ Distance calculation}
4.	$\Lambda_t \leftarrow d_t(s,v)$ **end for**	{ Update the index set}
5.	$\min_{c \in c^{\Lambda_t}} \Lambda$	{Select minimum row of the coefficient vector "C"}
6.	return t	{return the selected row number}

CHAPTER 4

EXPERIMENTS AND RESULTS

4.1 Overview

Up to now the hardware used in this study have been introduced. For modeling a target, a dipole model was applied. Minimum Euclidean Distance (MED) method was selected for this study to identify, localize and sequential localize a target. Since the aim of this study is setting up a sparse network, determining an efficient sensing zone for each sensor by practical experiments is a critical point for us. As expressed later each sensor has its own sensing orientation. During this chapter the results of sensor orientation, sensing coverage is shown. The undesirable effects such as temperature, magnetic noise, power supply level variation, direct sunlight are inspected.

Magnetic change curves when a target moves around the sensor for different paths are shown. The method which is used for creating a localization dictionary and identification dictionary is introduced. The results of identification of five targets for different entrance cell(s) are compared with each other. It follows by results of target localization for 4 discretization and 32 discretization form of the sensing region. To check the accuracy of the sensors and ILS system a network with nine sensors was set up. During a discrete movement the reaction of the sensors and performance of the Minimum Euclidean Distance (MED) method was considered. The results of this experiment clarified the well function sensors and the requirements for improving the code in order to have reliable estimations. A MATLAB code which is combined with minimum distance method was used for demonstrating the movement path of a target on network. For continuous movement a network with three reliable sensors was set up. The path estimation results are shown at the end of this chapter.

4.2 HMC1002 Axis Orientation

As we discussed in chapter 2.4 and 2.6.4 HMC1002 is 2-axis sensor and it can sense the magnetic field changes in 2 orthogonal directions. During the experiments we found that the axis direction suggested in HMC1002 datasheet [22] does not match with some of our sensors

directions. For identifying the correct direction of each sensor a series of tests have been done, using the two methods which we explained in chapter 2.6.4. The standard axis direction for HMC1002 is shown in Figure 4.2.a, and in Figure 4.2.b the Sensor Axis Orientation detector instrument is displayed which has been designed and fabricated by our team. Operation of this instrument is explained in details in section 2.6.4. The results of determining the magnetic sensors orientation are shown in Figure 4.3.c.

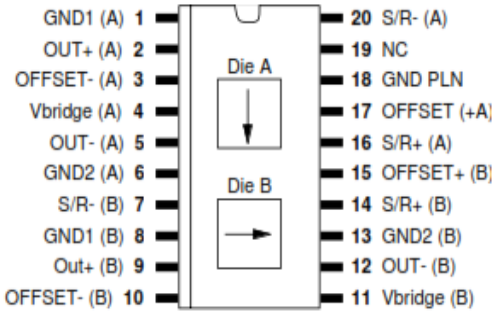

Figure 4.2.a: Standard axis orientation of HMC1002 Two-Axis magnetometer[22]

Figure 4.2.b: Axis orientation detector

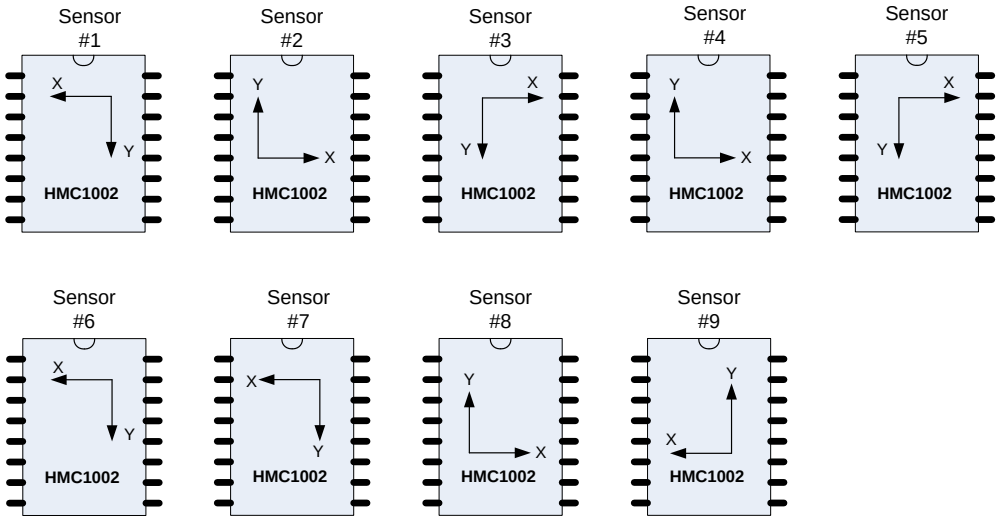

Figure 4.2.c Axis orientation of available HMC1002 sensor in CNG[2] laboratory

2: communication network group-department of EEE –METU – Ankara –Turkey

4.3 Sensing Coverage

In our ILS system the first step is identifying a target. Identification process should be operated at border of sensing region of each sensor, for this purpose we should know the maximum sensing coverage of each sensor. On the other hand we assumed that we have a sparse network. By this assumption the sensor sensing coverage's should not intersect with each other during the movement of a typical ferromagnetic object. During the movement, a target should be located at sensing region of just one sensor. By considering the limited number of the sensor for covering an area, noticing the sensor coverage domain enables us to distribute the sensors on the monitored area optimally. In this way our sensors will cover maximum area with the smaller number of sensors and minimum blind-zone area among them. It was determined that the sensor coverage area completely dependents on two parameters, the first one is the sensitivity of the sensor and the second one is the target characteristic such as shape, size, alloy, magnetic characteristic and etc. In order to Figure out how the distance and magnetic characteristic of the target effect on sensing issue, we setup a test with three targets different in size, shape and alloy. For achieving this unknown parameter we constructed a region as shown in Figure 4.3. It is essential to know the magnetic field disturbance is almost undetectable for AMR sensors beyond a specific distance. Also for closer distances the collected data from the sensors are not reliable. Sensor number three was placed at center of the circle. We initiated to make the target close to the sensor in zero degree angle. Simultaneously magnetic flux variation was monitored during this displacement. This part of experiment was performed for available targets in each direction with different angles. External border of sensing region is determined when the sensor started to report the first magnetic flux changes. After sensing the target, movement was continued in straight path as before toward the sensor. In too close distances the sensor goes to saturation mode and sends wrong data. During the movement toward the sensor when we received this type of data from sensor it means that we catch the minimum sensing boundary for that sensor and this is the internal sensing border. The results of sensor coverage for three different targets are shown in table (4.1)

Table 4.1 inner and outer sensing borders for magnetic sensors

Target	Target type	Minimum coverage	Maximum coverage
Target -1	Homogeneous – very small	7.5 cm	35 cm
Target -2	Homogeneous – small	10 cm	60 cm
Car	Composite – very large	1m	3m

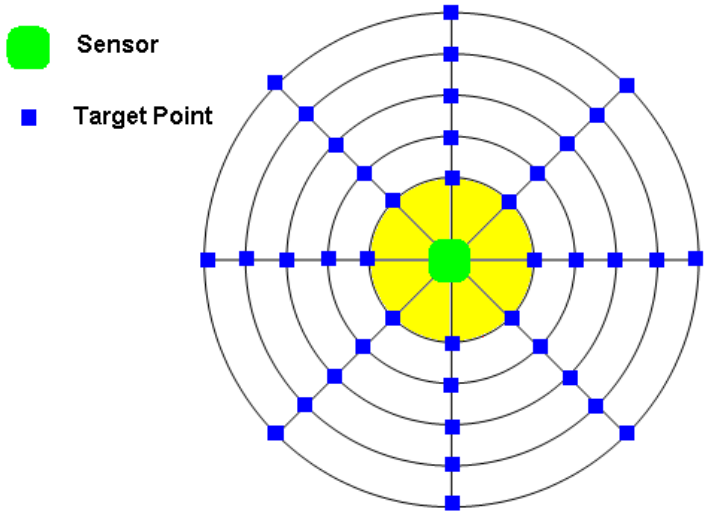

Figure 4.3 Defining inner and outer sensing region of the sensor. The yellow region is undetectable region and target should not enter this region

4.4 Effect of Temperature on Magnetic Measurements

In some applications, ILS system may be used in outdoor situations, so environmental variations like temperature, sunlight, etc may impress on measurements in the course of a day. To observe the effect of the temperature and also effect of direct sunlight on the magnetic sensors, an inspection was carried out at noon on April 29,2012 for 30 minutes from 11:45 up-to 12:30 in front of Building C of EEE department of METU. For providing a semi-isolated place of sensor in order to reduce the effect of wind, a sensor was situated in a cardboard box which has a removable cap. The test interval (30 minutes) was divided to two equal intervals (two 15 minutes). At first 15 minutes the sensor was in the cardboard box and the cap was on the cardboard box under the sunlight and in the second 15 minutes the cap was removed and the sensor was under the direct sunlight. In first interval (1^{st} 15 minutes) since sensor was in a covered area, its environment temperature increased linearly under sunlight. By observing Figures 4.4.b and 4.4.c we can conclude that for this sensor the X-axis magnetic reading (ADC value) increased from 519 to 530 but the Y-axis magnetic reading (ADC value) shows a similar behavior but in the opposite direction from 530 to 520 for first 15 minutes. In second interval the cap was removed, so the sensor was under direct sunlight. Due to the spring winds, the sensor's environment temperature was not in fixed degree. Figures 4.4.b and 4.4.c show that at second interval there is a non-linear variation in measurements of X-axis and Y-axis. Magnetic readings (ADC value) of X-axis increase from 530 to 583 and Y-axis decreases from 520 to 482 quickly.

Figure 4.4.d illustrates the temperature variation during the course of the 30 minutes for X-axis and Y-axis. According to [17] MTS310 sensor board has a Panasonic ERT-J1VR103J thermistor

which was used for monitoring the environment's temperature during the test. Following approximation can be used for converting the mote's ADC output to degrees Kelvin [17].

$$T(K) = \frac{1}{a+b\times\ln(R_{thr})+c\times[\ln(R_{thr})]^3} \quad (4.1)$$

where:

- Rthr = R1(ADC_FS – ADC)/ADC (4.2)
- a = 0.00130705
- b = 0.000214381
- c = 0.93×10^{-7}
- R1 = 10 KΩ
- ADC_FS = 1023
- ADC = Mote's ADC measurement for temperature
- For converting Kelvin degree to Celsius following equation can be used [32]:

$$[°C] = [K] - 273.15 \quad (4.3)$$

These results show that AMR sensors are very sensitive to variations of the temperature. For outdoor and also indoor applications the sensors should be located in a place which has minimum temperature variations. Fabricating a box which possesses the stable temperature condition and accommodating the sensor in that box is may be useful for eliminating the effects of temperature variation on the sensor. Since in ILS system the magnetic field change is considered, we purpose to update the ambient value in software automatically when there are any changes in temperature. These updates can increase the performance and accuracy of the readings.

Figure 4.4.a Magnetic sensor is located under the sunlight for studding the effect of temperature variation on AMR sensor

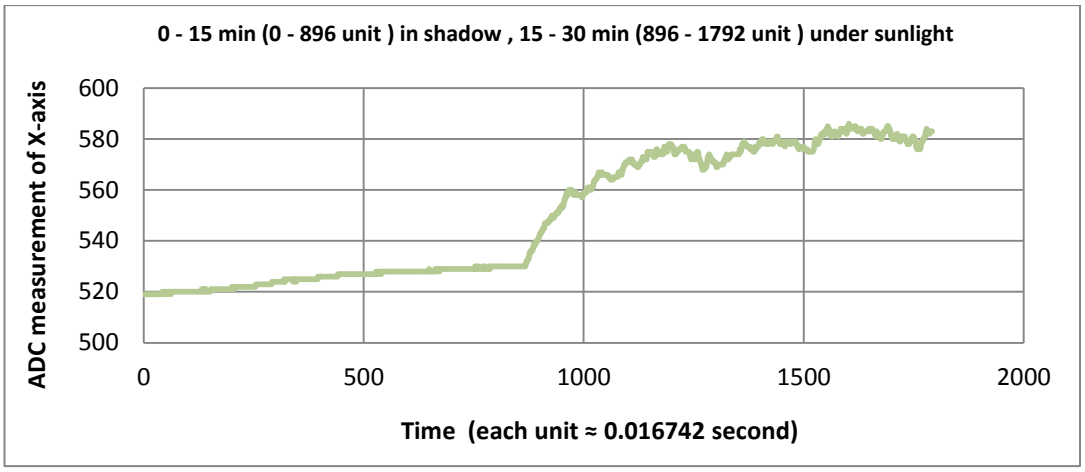

Figure 4.4.b X-axis magnetic readings in course of 30 minutes in shadow and under sunlight

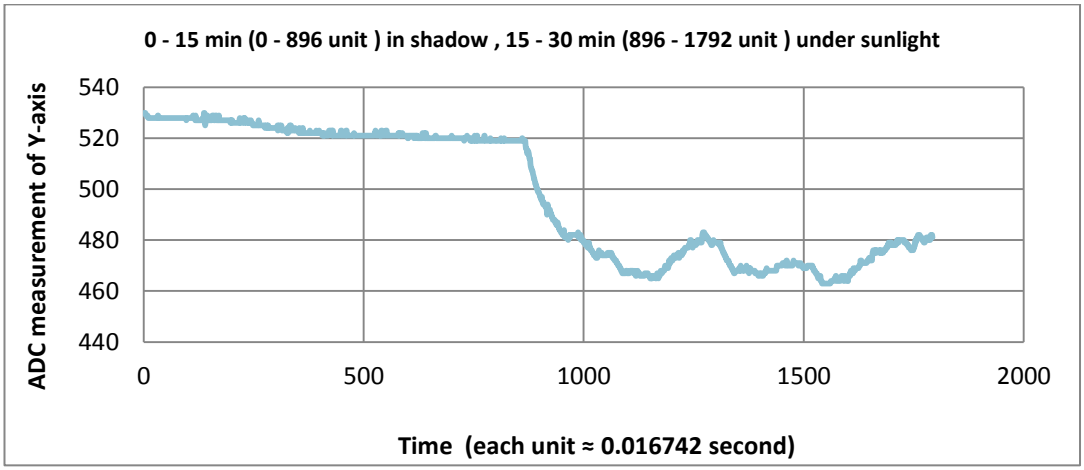

Figure 4.4.c Y-axis magnetic readings in course of 30 minutes in shadow and under sunlight

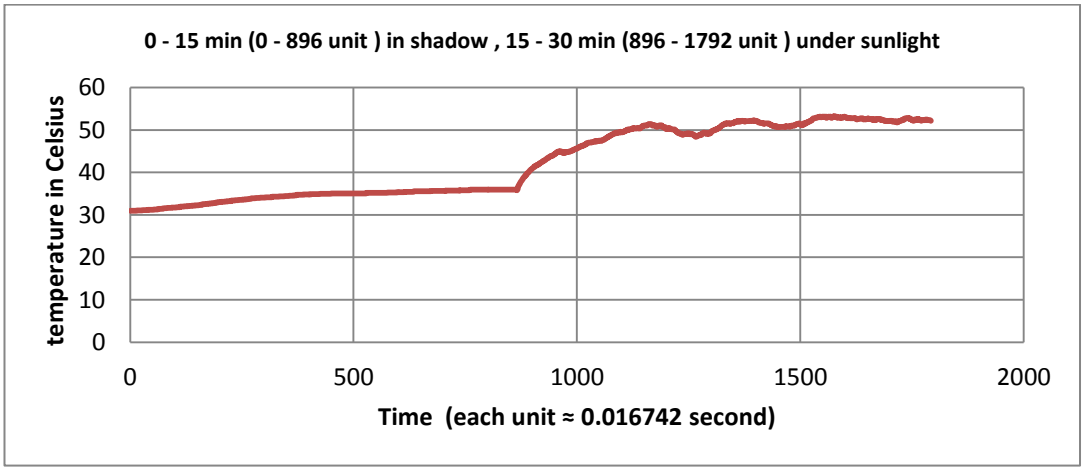

Figure 4.4.d Temperature variation in course of 30 minutes

4.5 Effect of Sunset on Magnetic Measurements

During the experiments usually in the evening we encountered with unknown variation in measurements. For detecting this unknown effect before initiating the experiment, the hardware and software were inspected several times. An air-conditioner was used for adjusting the temperature of the laboratory in a fixed degree. The motes were re-set up with new batteries. A vacation day was selected for test day, since noiseless environment (Free of magnetic noises) is essential for this test. Two sensors were applied in this test. These two sensors are located at different position in the laboratory. This experiment was conducted on Tuesday, May 1, 2012 at 17:30 – 20:30. Sunset time was 19:43 [29]. A significant magnetic field change was observed on measurement of the sensors in X and Y directions. This changes for both sensors in X and Y axis is illustrated in Figure 4.5. According to collected data after sunset time (19:43) a stable status can be seen for magnetic field. Updating the ambient value in software of the ILS system automatically in short periods, during the sunset and sunrise hours, could be a suitable solution for reducing this undesirable effect.

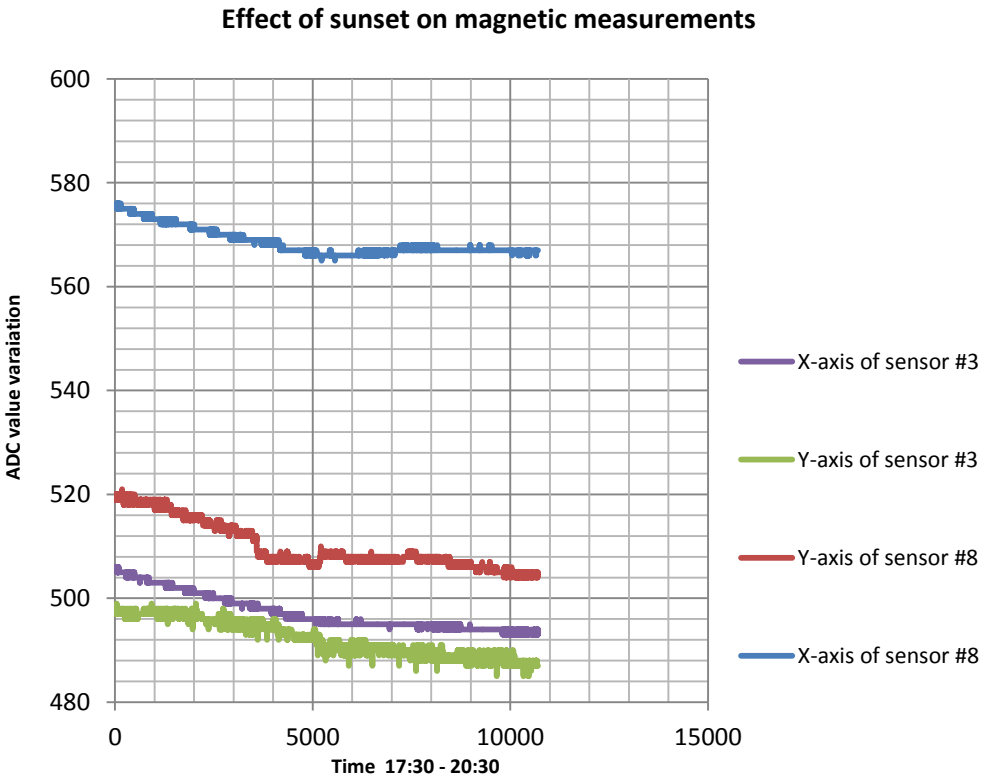

Figure 4.5 Effect of sunset on magnetic measurements

4.6 Effect of Power Supply Level on Magnetic Measurements

To know the effect of the power supply level on measurements a test was set up. An air-conditioner for stabilizing the temperature of the laboratory on fixed degree was utilized. The test was done in weekend in order to have minimum magnetic noises which were generated by passing cars or movable ferromagnetic objects. This test was done in a short time interval.

A DC power supply was used instead of two AA batteries (Figure 4.6.b). For different voltages from 3.2 V to 2 V, the magnetic intensity of the laboratory was measured. Figure 4.6.a shows the effect of these voltage variations on measurements of X and Y axis of sensors on HMC1002 magnetometer.

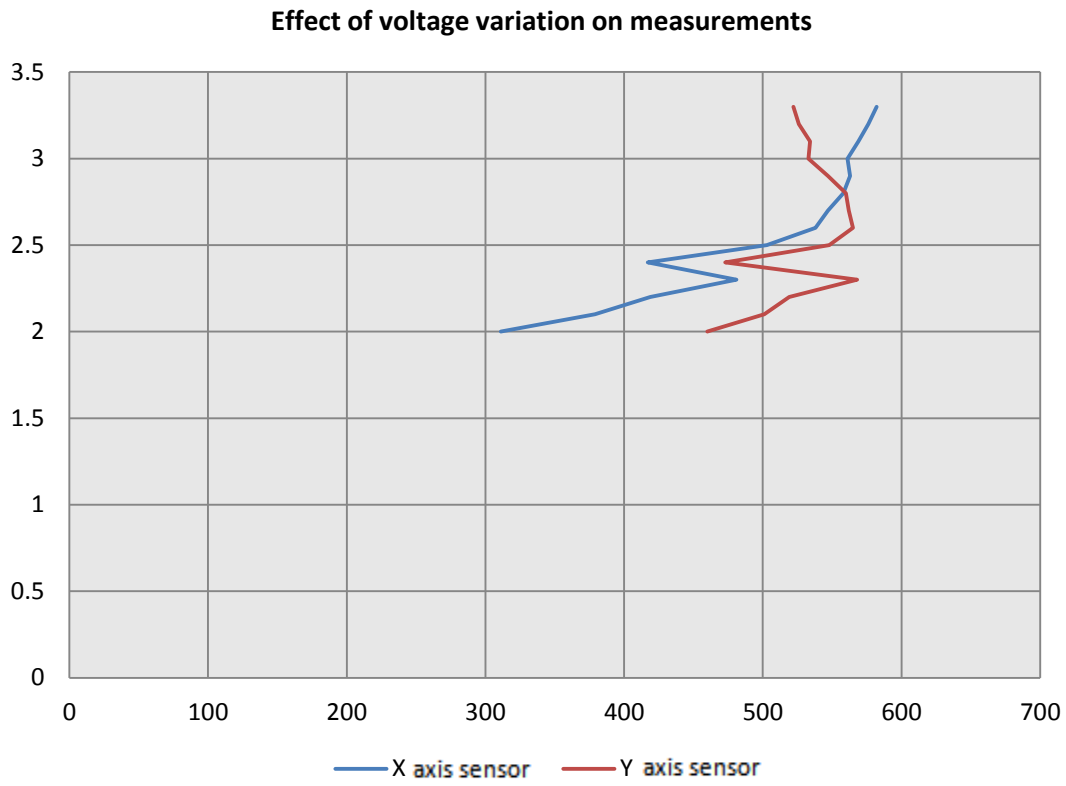

Figure 4.6.a Effect of voltage variation on magnetic measurements of HMC1002 in two axis

Figure 4.6.b A DC power supply provides the power of the sensor

In other to test the ambient magnetic field (B_{XA} and B_{YA}) and magnetic field of target at distance R from sensor (B_{XT} and B_{YT}) for different voltages was measured.
Results show that the subtracted value of these two modes (B_{XT} - B_{XA} and B_{YT} - B_{YA}) are fixed for different voltages.

Table 4.2 Comparison of the subtracted value of the ambient and target existence mood for different voltages for two AMR sensors on X and Y axis of the HMC1002 magnetometer

	B_{XA}	B_{YA}	B_{XT}	B_{YT}	B_{XT}-B_{XA}	B_{YT}-B_{YA}
3volt	581	569	591	664	10	95
2.8 volt	572	579	583	672	11	93
2.7 volt	567	481	579	575	12	94

4.7 Effect of Noise on Magnetic Measurements

In order to inspect the effect of unpredictable magnetic noise on measurements, an experiment was planned. A network with two sensors (sensor number 1 and 4) was set up. The small type of target was assumed for this test, so the area of the sensor sensing region is a circle with radius

30cm. The sensors were distributed on a sidewalk under the shadow of the bus station roof. A typical car is composed of different ferromagnetic materials so it can cause a specific disturbance on magnetic field of the earth around itself. This magnetic field is sensible by AMR sensors. By considering these explanations, passing cars and buses are assumed as unpredictable magnetic noises. The test time interval was 10 minutes. In this range, different kind of cars crossed but there was not any entrance to the assumed sensing region (a circle with radius 30cm).Curve of the collected data shows huge magnetic intensity changes when any car passes. In the following section and specifically in section 4.12.2 some solutions for reducing the undetectable noise have been purposed. Figure 4.7a and 4.7.b show curve of the collected data for sensor 4 in X and Y direction.

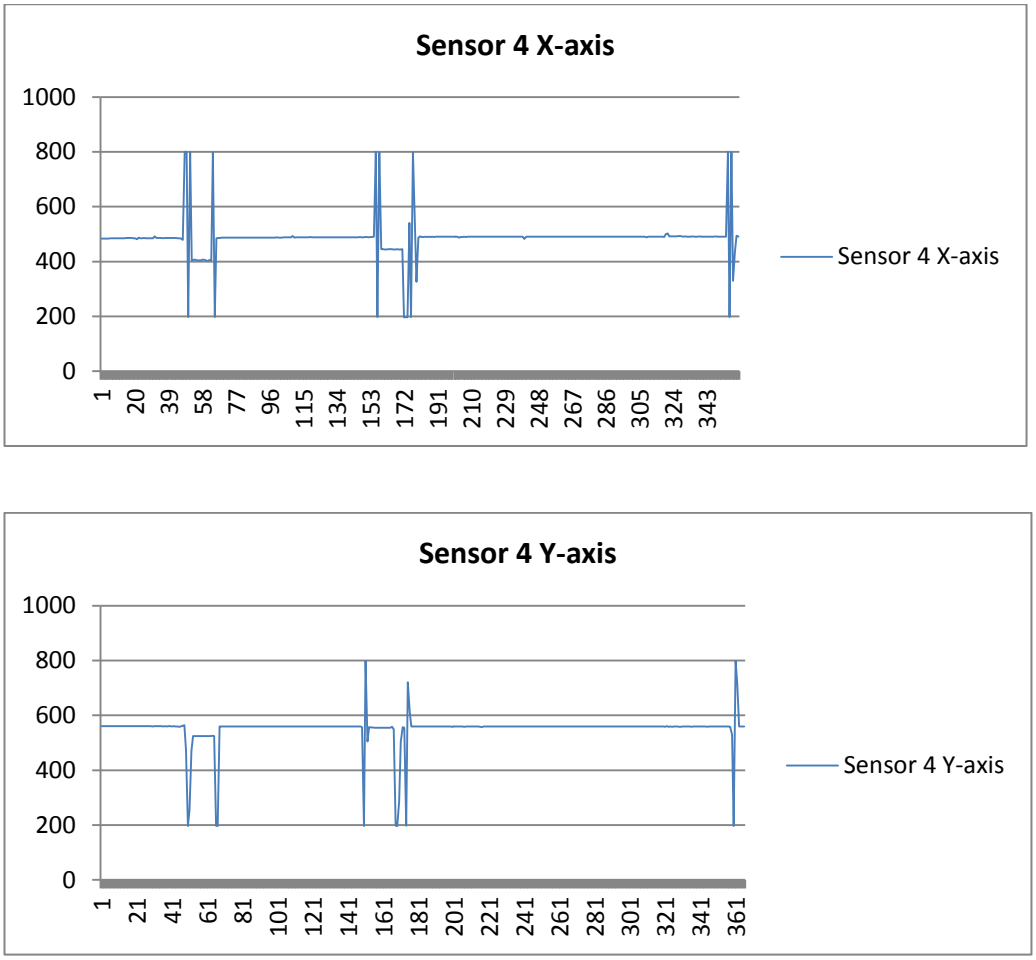

Figure 4.7 The collected data of sensor 4 was plotted to show the noise effect

4.8 Discrete Movements and Figure of Magnetic Field Changes

In this part of the study we tried to observe the change of magnetic field when a specific target (target number 3) passes in a known path. As shown in Figure 4.8.a the sensor was located at the center of the five concentric circles. The radii of the circles are 10cm, 15cm, 20cm, 25cm and 30cm. At each step of the test the target was located on the red points on a specific path. This target movement was from outer circle to inner circle and then in opposite direction from inner circle to outer circle. As clarified in previous parts, magnetic noise such as a movement of ferromagnetic object or entering and exiting a car in the experimental zone and also variation of the temperature may affect the measurements. For omitting the effect of these items, at each step before locating the target in a position, the magnetic felid of the environment was recorded for both of the X and Y axis (we named them BxA and ByA), then the target was located in determined positions and again magnetic field was recorded for both of the X and Y axis (we name them BxT and ByT). The difference between these two values shows the effect of the target from that point on the sensor. These tasks have been done for all of the red points. The magnetic field changes for each path are shown in Figures 4.8.b, 4.8.c, 4.8.d, 4.8.e.

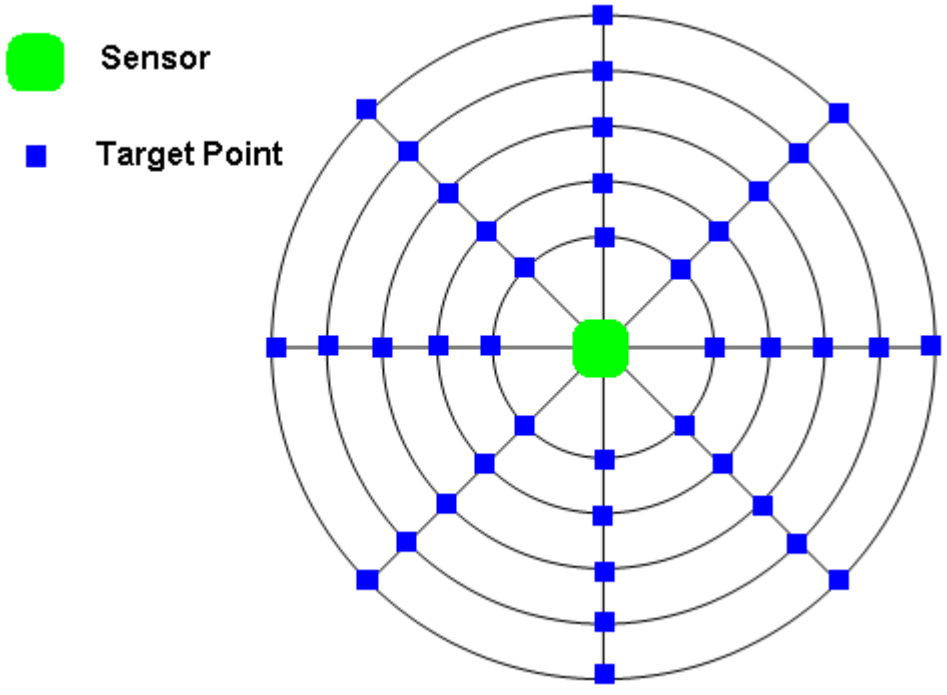

Figure 4.8.a Paths of discrete movement

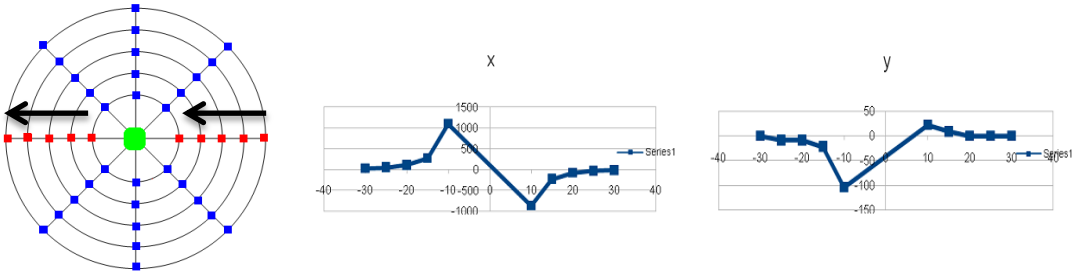

Figure 4.8.b Path of discrete movement on angle 0 – 180. Figure of magnetic field changes

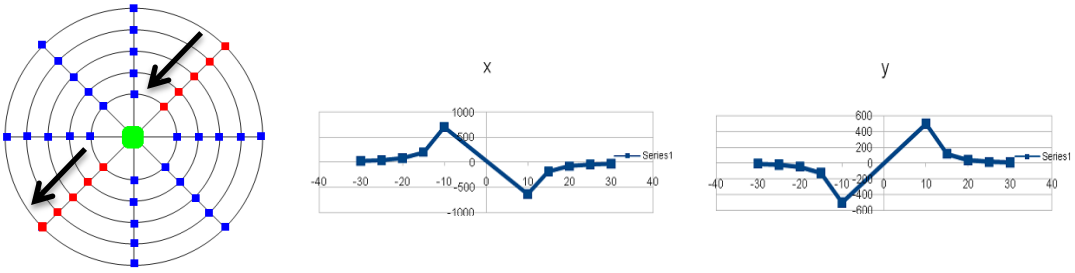

Figure 4.8.c Path of discrete movement on angle 45 – 225. Figure of magnetic field changes

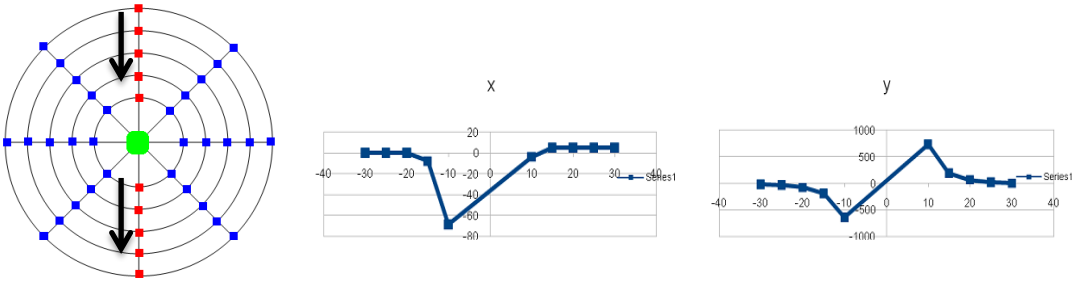

Figure 4.8.d Path of discrete movement on angle 90 – 270. Figure of magnetic field changes

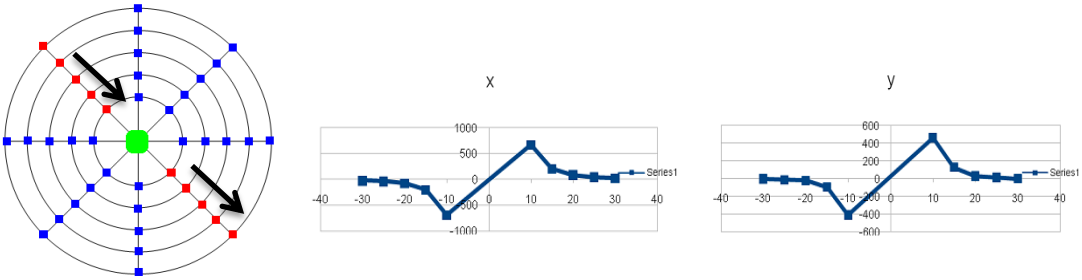

Figure 4.8.e Path of discrete movement on angle 135 – 315. Figure of magnetic field changes

4.9 Minimum Euclidean Distance (MED) Method for ILS System

As explained in the previous chapters, the first aim of ILS system is detecting, identifying, localizing and finally sequential localizing a ferromagnetic target in a defined wireless sensor network. By considering the previous parts, MICAz motes could be good solution for detecting the existence of a ferromagnetic target in the monitoring area. In general, detecting a target without knowing the position of the target is not very productive. In this work we attempted to use magnetic sensors in WSN for identifying the ferromagnetic targets (Target identification) and then estimating the location of the target in the sensible region of the sensors (target localization).

Different algorithms are offered by researchers for ILS systems. In this study Minimum Euclidean Distance (MED) method is used in ILS system. Orthogonal matching pursuit (OMP) algorithm for the first time is proposed for WSN as one of the future work of our research team to identify, localize and sequential localize a ferromagnetic object. The operation of the MED method for identification, localization and sequential localizing in ILS system will be expanded in the rest of this chapter. Test results show that, identification of a ferromagnetic target and location of that can be estimated by minimum distance method. Minimum Euclidean Distance (MED) method was introduced in chapter 3. OMP algorithm will be introduced in chapter 5.

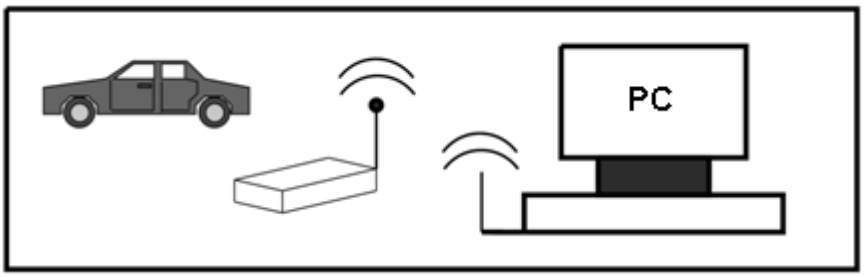

Figure 4.9.a An ILS system

4.9.1 Creating a Dictionary for MED Method

For using MED a dictionary should be created. First of all the sensor sensing region was discretized to 36 equal square cells. By clarification in section 4.3 each sensor has an inner and outer border for sensing. For small and very small targets, inner and outer radii are around 10cm and 30cm. By paying attention to these limitations, 28 cells were selected as target points for MED method (Figure 4.9.b). In initial step for each test point, magnetic field was measured for following situations separately:

- When there is no target at that point (for cell i we have B_{xAi} and B_{yAi}).
- When a specific target at that point (for cell i we have B_{xTi} and B_{yTi}).

The difference between these two values for each axis shows the effect of the target from that test point on the sensor on that axis.

$$\Delta B_{xi} = B_{\mathrm{xTi}} - B_{\mathrm{xAi}} \tag{4.4}$$

$$\Delta B_{yi} = B_{\mathrm{yTi}} - B_{\mathrm{yAi}} \tag{4.5}$$

The value of the equations 4.4 and 4.9 are i^{th} row of the dictionary for MED. i^{th} row is named φ_i.

$$\varphi_i = [\Delta B_{xi} \quad \Delta B_{yi}] \tag{4.6}$$

By considering these explanations the dictionary for MED can be defined as follows:

$$\mathrm{D} = [\varphi_1 \ \varphi_2 \ \dots \ \varphi_I]^T \tag{4.7}$$

Where "I" is the number of the test point. For this case I=28

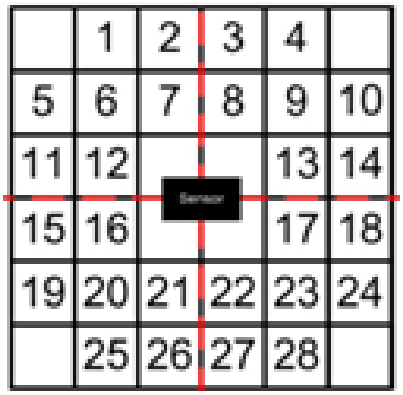

Figure 4.9.b Sensor sensing region discretization

4.10 Target Identification and MED Method

As explained in section 4.3 each sensor has its own sensing coverage which depends on the magnetic characteristic of the monitored target. To increase the performance and decrease the running time of the MED method, separate dictionaries were generated for different targets. Identifying the target and then using the related dictionary during the tracking is an important step for ILS system. It is a good idea to identify the target in outer border of the sensor coverage in order to define which of the dictionaries should be used in tracking phase. During this section different entrance gateway to sensing region of a sensor is considered.

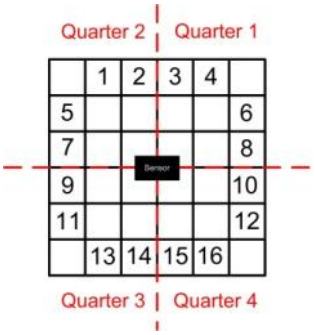

Figure 4.10.a Two different form of discretization of sensor sensing region

To apply MED method in ILS system a dictionary is required. In order to create a dictionary for Identification, the sensing region of the sensor number 11 was discretized to equal cell. For checking the accuracy of the MED in identification mode, small and very small type of targets was selected for following. It means that the distance between outer sensing band and sensor is 30cm. The position of the sensor was selected at the center of a square with the area of 3600 cm^2. In one case this area was discretized to 36 square cells with length of 10cm and in the other case to 4 square cells with length of 30cm as shown in Figure 4.10.a. In first case the cells which are on the border of sensing region were used of generating the dictionary and in second one all of the four cells were selected as target position for generating the dictionary. In following sub-sections we will compare the different form of discretization and target entrance points.

4.10.1 Sixteen Cells on the Border - Unknown Entrance Point

In this case the border of the sensing region was discretized to 16 cells and MED method was used in order to identify the target. For creating an identification dictionary, firstly magnetic field of the sensor region was measured when there was no ferromagnetic object in that region. Then target number N (N=1, 2, 3, 4, 5 …) was placed in the cell number i and again magnetic field of the sensor region measured. The difference between two measurements shows the magnetic effect of that target from the cell number "i" on intended sensor. This value was selected as an entry for row number [(N-1) ×16] + i of the Identification dictionary. Where N is target's number and i is the cell's number. These tasks were repeated for all of the 16 cells and all of the targets. Since in each measurement we collect data from X and Y axis so there are two entries in each row of the identification dictionary.

The number of row in identification dictionary completely depends on the number of the targets and number of the cells in outer border of the sensing region. For this test, equation 4.7 should be changed to:

$$D = [\varphi_{1,1}\ \varphi_{2,1}\ \dots\ \varphi_{I,1} \dots \varphi_{1,2}\ \varphi_{2,2}\ \dots\ \varphi_{I,2}\ \dots\ \varphi_{1,N}\ \varphi_{2,1}\ \dots\ \varphi_{I,N}]^T \quad (4.8)$$

where I is the number of the test point and N is the number of the targets. For this case I=16 and N=5.

Test number 1 was run with five targets when border of the sensing region was discretized to 16 equal squares as Figure 4.10.b. Target entrance point could be any of these 16 cells so it is unknown for MED method. This test was done in 2 runs for five targets.

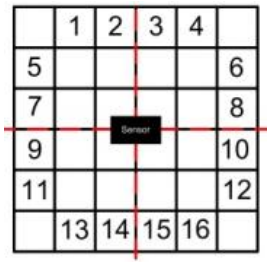

Figure.4.10.b Sensor sensing region discretization for unknown entrance point and 16 cells on the border

Table 4.3 Target identification / 2 run / 16 cell / 160 observation / 5 targets

result	Count	Percent %
Correct	77	48
Wrong	83	52

In this test after creating a dictionary, all of the targets located in the entire test points one by one in two runs. Therefore, we have 160 observations for this test (5 ×16 × 2 = 160). According to the results with %48 target identification can be done by MED algorithm.

Table4.4 Confusion matrix for unknown entrance point (16 cells)

Confusion matrix 2 test / 160 data		Target estimation				
		i	ii	iii	iv	v
Target	i	18	2	5	5	2
	ii	5	15	5	6	1
	iii	5	4	12	8	3
	iv	6	4	4	18	0
	v	2	6	5	4	15

4.10.2 Known Entrance Point (One Cell)

For second case, identification dictionary was created for 5 targets for a cell. The equation 4.7 should be modified in this form:

$$D = [\varphi_{C,1} \ \varphi_{C,2} \ \dots \ \varphi_{C,N}]^T \tag{4.9}$$

Where C is the cell's number and N is the number of the Targets. For this case C=1 and N=5.

This test was done in four runs. Five targets were put in cell number 1 one by one. Number of the observation was 20 (4 × 5 × 1 = 20) the results show that we can identify the targets exactly if the observation region (test point) is fixed for all targets.

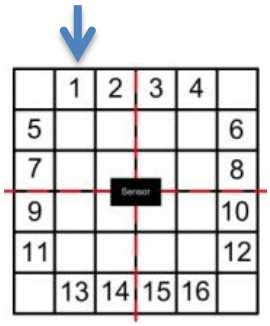

Figure 4.10.c Sensor sensing region discretization for known entrance point (one point)

Table 4.5 Target identification / 4 runs / 1 cell / 20 observation / 5 targets

result	Count	Percent %
Correct	20	100
Wrong	0	0

Table 4.6 Confusion matrix for known entrance point (one cell)

Confusion matrix 4 test / 20 data		Target estimation				
		i	ii	iii	iv	v
Target	i	4	0	0	0	0
	ii	0	4	0	0	0
	iii	0	0	4	0	0
	iv	0	0	0	4	0
	v	0	0	0	0	4

4.10.3 Known Entrance Point-Four Cells in the Same Quarter

For this test, target entrance region was restricted to four sub-regions as Figure 4.10.d. It means that the test regions for target identification are 1,2,5,7 (border of the 2nd quarter of the sensing square is selected as entrance points).

In this test, identification dictionary was created for 5 targets when there are four cells for entrance point. The equation 4.7 should be modified in this form:

$$D = [\varphi_{C,1} \ \varphi_{C,2} \ \dots \ \varphi_{C,N}]^T \quad (4.10)$$

Where C is the cell's number and N is the number of the Targets. For this case C=1, 2, 5, 7 and N=5

This test was done in two runs. Five targets were put in cells number 1, 2, 5 and 7 one by one. Number of the observation was 40 (2 × 5 × 4 = 40). Following results were obtained for this case.

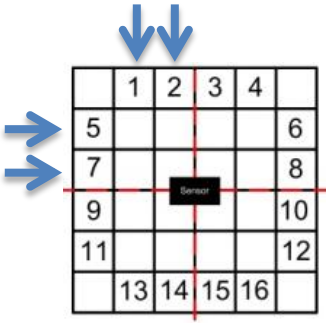

Figure 4.10.d Sensor sensing region discretization for known entrance point (four cell in the same quarter)

Table 4.7 Target identification / 2 runs / 4 cell in the same quarter/ 40 observation / 5 targets

result	Count	Percent %
Correct	29	72
Wrong	11	28

Table 4.8 Confusion matrix for known entrance point (4 cell in the same quarter)

Confusion matrix 2 test / 40 data		Target estimation				
		i	ii	iii	iv	v
Target	i	7	0	0	1	0
	ii	3	3	0	2	0
	iii	0	0	6	0	2
	iv	2	0	0	6	0
	v	0	0	1	0	7

4.10.4 Known Entrance Point-Four Cells in Different Quarters

For this test four sub-regions in different quarters were selected for target entrance point as Figure 4.10e. Cell number 8 in quarter 1, cell number 2 in quarter 2, cell number 15 in quarter 3 and cell number 9 in quarter 4.

In this test, identification dictionary was created for 5 targets when one entrance point was selected from each quarter, so in total, there were four gates for this experiment. Dictionary of this section is like the dictionary of the previous section just with different cell numbers:

$$D = [\varphi_{C,1} \ \varphi_{C,2} \ \dots \ \varphi_{C,N}]^T \tag{4.11}$$

where C is the cell's number and N is the number of the Targets. For this case C=8, 2, 9 and 15 and N=5

This test was done in two runs. Five targets were put in cells number 8, 2, 9 and 15 one by one. Number of the observations was 40 ($2 \times 5 \times 4 = 40$). Results of this case:

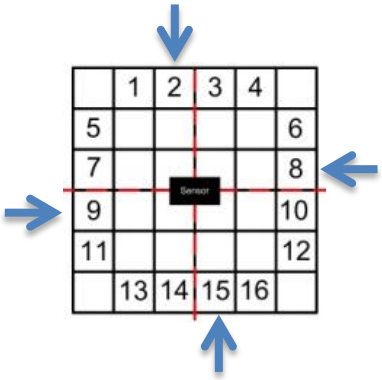

Figure 4.10.e Sensor sensing region discretization for known entrance points (four cells in different quarters)

Table 4.9 Target identification / 2 runs / 1 cell / 40 observation / 5 targets

result	Count	Percent %
Correct	27	67
Wrong	13	33

Table 4.10 Confusion matrix for known entrance point (4 cell in different quarters)

Confusion matrix 2 test / 40 data		Target estimation				
		i	ii	iii	iv	v
Target	i	6	1	1	0	0
	ii	0	8	0	0	0
	iii	1	3	3	0	1
	iv	3	0	1	4	0
	v	0	0	2	0	6

4.10.5 Known Entrance Point - One Cell – One Target and Inverted Form of That Target

In this experiment the magnetic property of a target is investigated. Cell number 2 was selected for target entrance point as Figure 4.10f. In this test, identification dictionary was created for one target. Cell number two was selected as the gateway of the target for this experiment. The equation 4.11 should be modified in this form:

$$\mathrm{D} = [\varphi_{C,1} \;\; \varphi_{C,2} \;\; \dots \;\; \varphi_{C,N}]^{T} \qquad (4.12)$$

where C is the cell's number . For this case C=2.

This test was done in two runs. Target number 3 was located in cells number two and then inverted form the target 3 was located in the same cell. Number of the observation was 4 (2 × 2× 1 = 4).

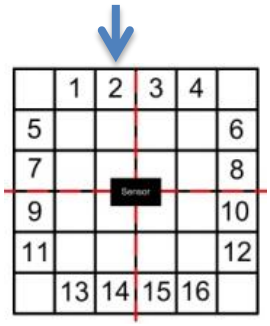

Figure 4.10.f Sensor sensing region discretization for known entrance point one cells – one target and inverted form of that target

Table 4.11 Target identification / 2 runs / 1 cell / 4 observation / 1 targets but in 2 form

result	Count	Percent %
Correct	2	50
Wrong	2	50

The result of this test shows that when a ferromagnetic object inverted, its magnetic properties are changed. It means that inverted target is a new target which should have its own dictionary in ILS system.

4.10.6 Known Entrance Point - One Cell – Two Similar Targets

This experiment was organized to generalize a target result to other the same targets. Cell number 2 was selected for target entrance point as shown in Figure 4.10f. In this test, identification dictionary was created for two the same targets. The equation 4.16 should be altered in this form:

$$\mathrm{D} = [\varphi_{C,Original\ Target}\ \ \varphi_{C,Similar\ target}]^{T} \qquad (4.13)$$

where C is the cell's number . For this case C=2.

This test was done in two runs. Target number 3 was located in cells number two and then replaced with a similar target. Number of the observation was 40 (2 × 2× 1 = 4). The results show that for the same targets, equal results can be obtained.

4.11 Target Localization and MED Method

In previous section different form of target identification was considered. Content of this section will focus on localization subject, since the position of a target is an important item for ILS systems. The method used in this study, is so similar to target identification which was discussed in previous sections. Minimum Euclidean Distance method is the main algorithm for target localization. Data collecting and dictionary creating is so similar to target identification.

For laboratory studies the sensing region of the sensors are discretized to 36 and 4 sub-regions (Figure 4.11.a and 4.11.b).

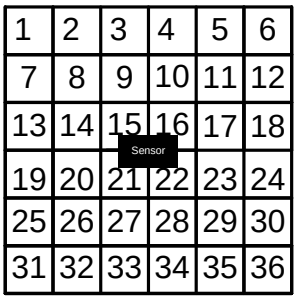

Figure 4.11.a 36 sub-region around the sensor

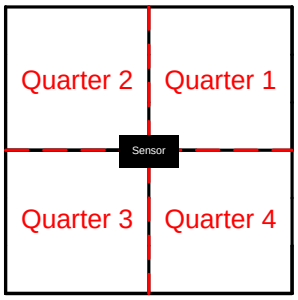

Figure 4.11.b 4 sub-region around the sensor

Since small and very small type of objects is used as a target in these tests, the sensing region of a sensor is a circle with radios 30cm. By considering this sensing region, in first case, 28 cells which are mostly in this coverage are selected as test points (Figure 4.11.c).

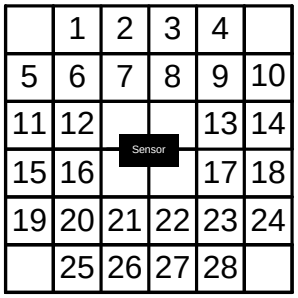

Figure 4.11.c 28 cells which are mostly in sensor sensing coverage.

Target localization was investigated in three cases, which has its own advantages and disadvantages. In following sub-sections these three cases will be introduced in details.

4.11.1 Localization With Resolution of 10cm × 10cm With 28 Data Points

The sensor sensing region is discretized to 28 equal squares (cells) with area of $100cm^2$ for each cell (Figure 4.11c). For creating a localization dictionary for a target, following tasks were done. Ambient of the region for X and Y axis of the sensor was measured (B_{x1A} and B_{y1A}). After that, a target is located at cell number one and magnetic intensity of the new environment for X and Y axis of the sensor was measured again (B_{x1T} and B_{y1T}). The difference of these two values demonstrates the effect of that target from the cell number one on the sensors. This value is the first entry of the localization dictionary. These tasks were repeated for remaining cells. Creating a dictionary for ILS system is explained in section 4.9.1 in details. For each target a different localization dictionary was generated. The test of "Localization with resolution of 10cm × 10cm with 28 data points" was done in two runs. In each run the localization of each target was investigated separately. Hence over all for this case 10 experiments were done. In the following tables the results can be seen. According to the following results with %74 the location of targets can be estimated correctly while the resolution of location estimation is 10cm × 10cm.

Table 4.12 Target localization results / resolution: 10cm × 10cm / 28 data points / 1st run

	First run / 28 cells / there 28 test point for targets									
	Target #1		Target #2		Target #3		Target #4		Target #5	
	Count	%	Count	%	Count	%	Count	%	Count	%
Correct	16	57	20	71	20	71	24	86	21	75
Near*	9	32	8	29	8	29	3	11	6	21
Wrong	3	11	0	0	0	0	1	3	1	4

Table 4.13 Target localization results / resolution: 10cm × 10cm / 28 data points / 2nd run

	Second run / 28 cells / there 28 test point for targets									
	Target #1		Target #2		Target #3		Target #4		Target #5	
	Count	%	Count	%	Count	%	Count	%	Count	%
Correct	14	50	22	78	24	86	21	75	21	75
Near*	11	39	5	18	14	5	5	18	7	25
Wrong	3	11	1	4	0	0	1	7	0	0

Table 4.14 All Targets localization / resolution 10cm × 10cm / 28 data points / 1st run

First run / 28 cells / all targets	
Correct	102
Near*	32
Wrong	6

Table 4.15 All Targets localization / resolution 10cm × 10cm / 28 data points / 2nd run

Second run / 28 cells / all targets	
Correct	101
Near*	34
Wrong	5

Table 4.16 All Targets localization / resolution 10cm × 10cm / 28 data points / all runs

Results of localization for 2runs/28 subregion/280 observation/5 target	
Correct	203
Near*	66
Wrong	11

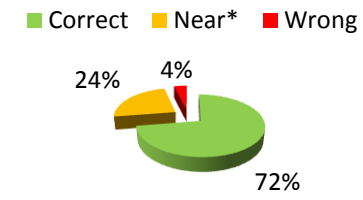

Figure 4.11.d Results of localization for 2runs /28 subregion /280 observation / 5 taget

*: the distance between the correct location and estimated location is not more than 10cm.

4.11.2 Localization With Resolution of 30cm × 30cm With 28 Data Points

In this case the sensing region of the sensor was discretized to 28 cells and localization dictionary generation was similar to the section 4.11.1. For this test the localization resolution was 30cm × 30cm. It means that each seven small cell made a new cell. In total there exist four new cells around the sensor. Figure 4.11.e illustrates this discretization. By using data of 28 cells the position of the target was estimated. In this case a quarter of the sensing region is considered. To clarify this, consider following example: if target is in cell number 8 and MED estimate the location of the target any of the cells number 3, 4, 8, 9, 10, 13, 14, it means that the location of the target is estimated correctly.

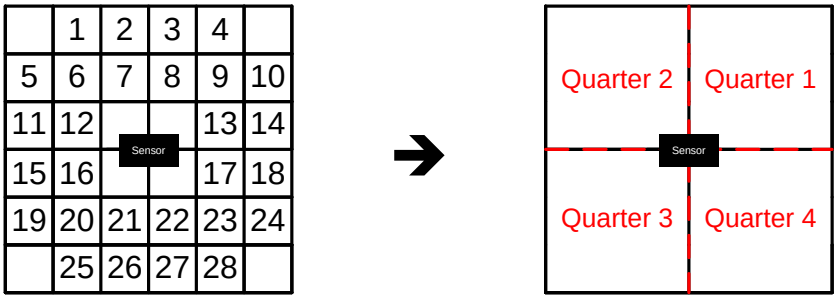

Figure 4.11.e Discretization for Localization with resolution of 30cm × 30cm with 28 data points

The test of "Localization with resolution of 30cm × 30cm with 28 data points" was done in two runs. In each run the localization of each target was estimated separately. So overall for this case 10 tests were done. In the following tables the results can be seen.

Table 4.17 Target localization results / resolution: 30cm × 30cm / 28 data points / 1st run

	First run / 4 cells / there 28 test point for targets									
	Target #1		Target #2		Target #3		Target #4		Target #5	
	Count	%	Count	%	Count	%	Count	%	Count	%
Correct	27	96	26	93	28	100	28	100	28	100
Wrong	1	4	2	7	0	0	0	0	0	0

Table 4.18 Target localization results / resolution: 30cm × 30cm / 28 data points / 2nd run

	Second run / 4 cells / there 28 test point for targets									
	Target #1		Target #2		Target #3		Target #4		Target #5	
	Count	%	Count	%	Count	%	Count	%	Count	%
Correct	27	96	27	96	28	100	27	96	28	100
Wrong	1	4	1	4	0	0	1	4	0	0

Table 4.19 All Targets localization / resolution 30cm × 30cm / 28 data points / 1st run

First run / 4 cells / all targets	
Correct	137
Wrong	3

Table 4.20 All Targets localization / resolution 30cm × 30cm / 28 data points / 2nd run

Second run / 4 cells / all targets	
Correct	137
Wrong	3

According to the following results with %98 the location of targets can be estimated correctly while the resolution of location estimation is 30cm × 30cm.

Table 4.21 All Targets localization / resolution 30cm × 30cm / 28 data points / all runs

Results of localization for 2runs/4 cells /280 observation/5 target	
Correct	274
Wrong	6

Figure 4.11.f Results of localization for 2 runs / 28 sub region / 280 observation / 5 targets

4.11.3 Localization With Resolution of 30cm × 30Cm With 4 Data Points

In the third form of target localization, the sensor sensing region was discretized to four equal cells with area of 30cm × 30cm for each cell. According to section 4.9, in this case for each target a dictionary with four rows was generated. This test was done in three runs. In each run the localization of each target was estimated separately. Therefore overall for this case 15 experiments were done. In the following tables the results can be seen.

Table 4.22 Target localization results / resolution: 30cm × 30cm / 4 data points

Results of localization for 3runs / 4 cells /60 observation/5 target	
Correct	60
Wrong	0

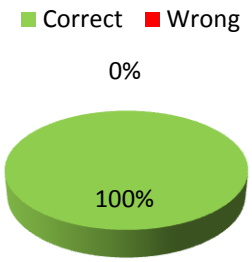

Figure 4.11.g Results of localization for 3 runs / 4 sub region / 60 observation / 5 targets

These results shows that if the sensing region discretized to four cell the location estimation can be done with high accuracy under fixed environment conditions. In this case the exact location of a target is not so essential, just the relative location of the target is considered.

4.12 Sequential Localization and MED Method

As seen in earlier chapters, MED method was determined a possible method for identifying and localizing a target on the network. Since the main aim of the ILS system is tracking or sequential localization of a target in its domain, the remaining parts of this chapter is devoted to this subject. Firstly discrete movement will be investigated in details and possibility of the MED method and proper functioning of the sensors for tracking a target will be checked. The obtained results will be used for continuous movements. A real ILS system will be shown. At the end, the path of a real continuous movement will be compared with the MED estimated path.

4.12.1 Sequential Localizing a Target With Discrete Movement

In order to check the performance of the MED method and accuracy of the sensors, a wireless network with nine sensors was set up (Figure 4.12.a). By these sensors a region with area of 240cm × 240cm was covered.

Figure 4.12.a A testbed with 9 sensors for tracking a target in discrete movement

According to the previous sections each sensor has a sensing region. Due to this fact, the sensing region of each target is discretized as Figure 4.12.c. The gaps between the sensors are for making a sparse network. The distance between the adjacent sensor sensing regions is 30cm. Since for this study a target should be at the sensing domain of one sensor at each movement, so

this gap guaranties this condition. By this clarification during the tests, among the collected data, the data of one sensor which had a variation was used for tracking at that moment.

In this network the sensor sensing region of each sensor is discretized to 28 cells. Two iron bars were selected as targets. (Target #2 and #5 Figure 4.12.b).

Figure 4.12.b Target number 2 and number 5

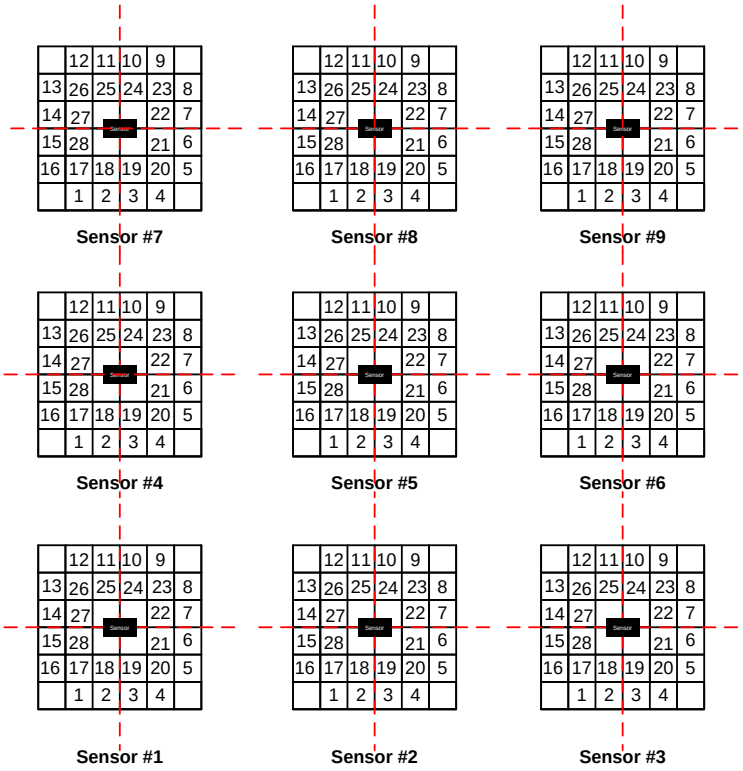

Figure 4.12.c Discretize form of the sensor sensing region for discrete movement

For identification, the cells on the outer border of the sensing region were selected for test points. For generating an identification dictionary for each sensor, the tasks of section 4.10.1 were done. Over all for this system, there were nine identification dictionaries which have (16 × N) rows and 2 columns, where N is the number of targets. Each column represents the flux density of each direction (X and Y). For this case N=2, so the identification dictionaries have 32 rows and 2 columns. First sixteen and second sixteen rows belong to target 2 and 5 respectively.

In order to increase the reliability of the system, on the outer border of the sensor sensing region target identification process is done. The result of this process will be used for target localization and finally for target sequential localization and tracking.

To generate localization dictionary for each sensor, the method of the section 4.11.1 was applied. For each sensor there is N localization dictionary with 28 rows and 2 columns where N is the number of the targets. In general, for ILS system the number of the localization dictionary is N × S where S is the number of the sensors in this system.

For creating dictionaries and also during the tests to minimize the error of the operation, data of the sensors were collected in 3 or 4 consequent, while the ADC value were read 8 times at each second for each sensor. At each moment there were 32 data package available for each sensor. As expressed previously magnetic sensors are so sensitive and measurements can be spurious. For increasing the accuracy of the collected data, mode of these 32 data packages were calculated. We name this form of selecting data "mode method". If the sensors function well and not depend to environment conditions, just one packet data is sufficient for MED method to identify and localize a target.

There is a guard band of 30cm between outer sensor sensing regions of two adjacent sensors. None of the sensors cannot sense any target at guard band, so we called this regions "blind zones". If a target exists on the monitored area, by considering sparse assumption for this experiment, there are two moods for target and coming data:

1. If a target located in blind zone, ILS system cannot sense existents of that. Collected data form each sensor are so similar to ambient data.
2. If a target located at sensing region of one sensor, collected data of that sensor must shows this event and data of remaining sensors have to be similar to ambient data.

Mood #2 shows that when a target is in the sensing zone of a sensor, data changes must be observed just on collected data of that sensor, otherwise some of the sensors are not operating well or there is more than one target in sensing region of the different sensors.

Following items can affect the ILS system measurements:

1. If sensors sensing region are overlapped, the location estimation cannot be accurate. Since a proper sensor and correct dictionary selection in not possible for ILS system.

2. If sensors do not operate well during the tests wrong data will be obtained. During the experiments we found out that some of the sensors were sending fake data when there was no target in sensing region of those sensors.
3. If magnetic flux density of the environment changes rapidly during the tests we will encounter with problem for estimating the location and identification

In order to check the MED method for identification in discrete movements, a random cell at border of each sensor sensing region was selected (4.12.d). Target #2 and #5 were placed at these test points one by one. The place of the target is not known for MED algorithm. It is the general form of the entrance to the network. As clarified in sections 4.10.2, if the entrance point is known for MED algorithm, ILS system can identify the target with no error if sensors work well and targets are different with each other. Following results were obtained for identification of two targets (target number 2 and number 5) while entrance cells were not known to MED:

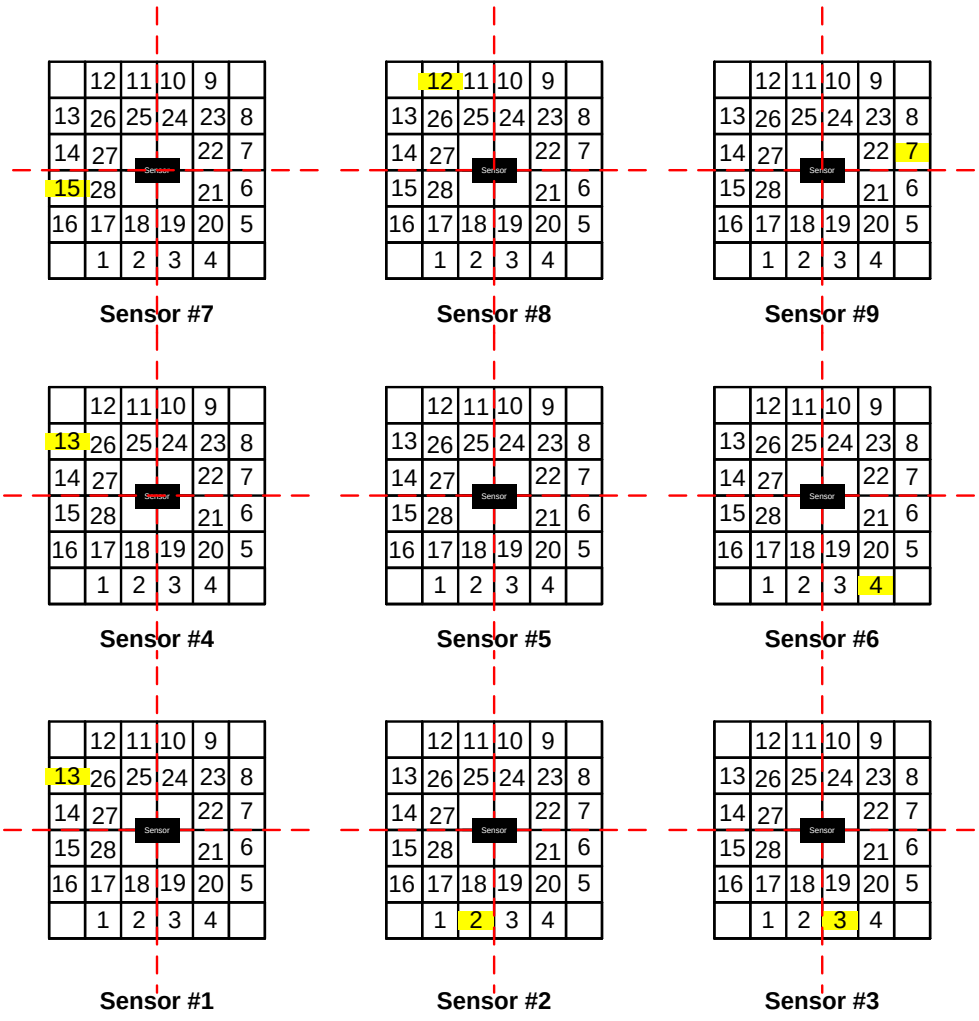

Figure 4.12.d Arbitrary test point on each sensor (yellow cells) for target identification

To investigate the operation of the MED algorithm for localization, target was known to MED algorithm. When a target was at sensing region of a sensor, data of that sensor was collected and function of the other sensors was under the control and observation. During the tests some of the sensors were not operating fine and some of the sensors were sanding fake data. In fact we set up discrete movements test for checking the function of the sensors and selecting the best ones for our ILS system in continuous movement. This part of the test was done in two runs. First with target number 2 and then with target number 5. Figure 4.12.e and 4.12.f illustrates the real discrete movement and estimated path for target #2 and #5 respectively. At first run target number 2 was selected. This target was placed in preselected test point. The collected data was used as the input of the MED algorithm. The estimated points and paths were plotted. These jobs repeated for target number 5 again. Table 4.24 shows the target location estimation results.

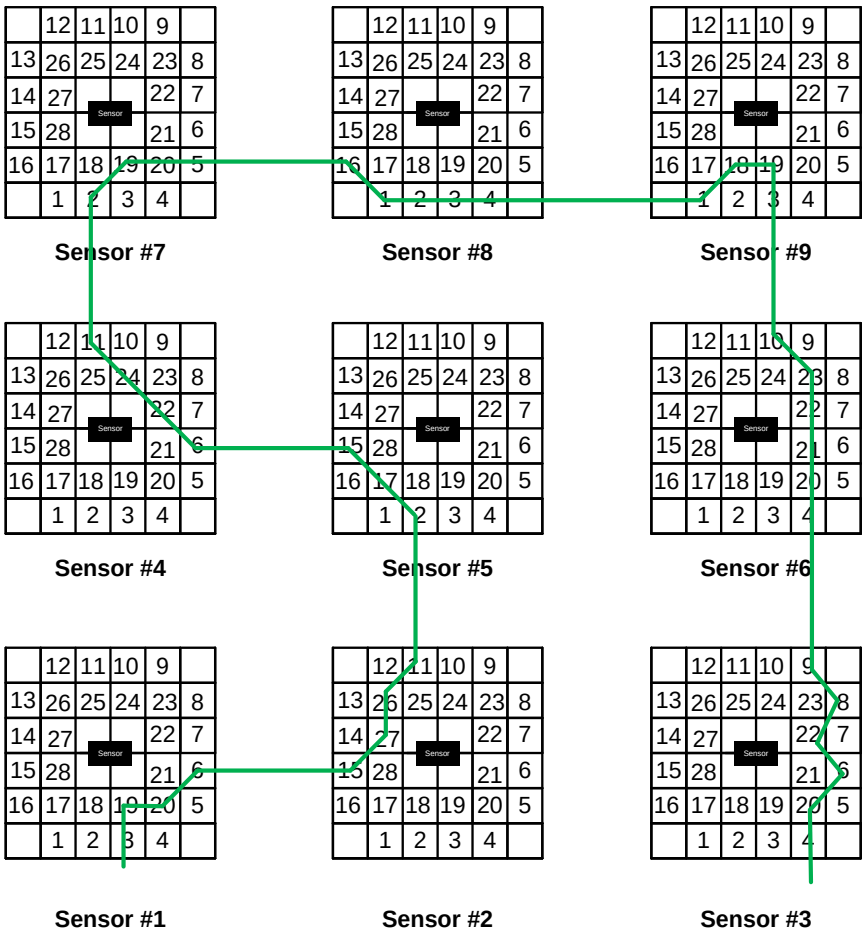

Figure 4.12.e Real path for discrete movement test

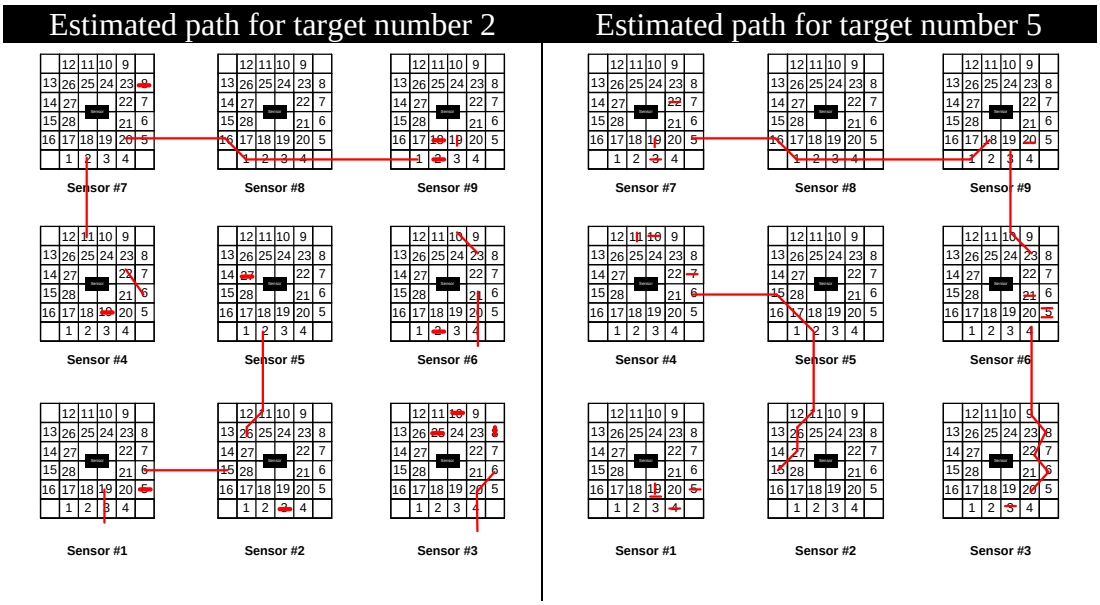

Figure 4.12.f Estimated paths for discrete movement of target #2 and #5

Table 4.23 Results of target localization for all targets for discrete movement

	Target 2	Target 5
Correct estimation count	29	28
Near estimation count	5	7
Wrong estimation count	6	5

As expressed, during the experiments some of the sensors did not have accurate measurements and sending fake data. The counts of sensor error for localization and identification tests are shown in following table. By considering these results suitable sensors were selected for continuous movements test.

Table 4.24 Count of sensor error during target identification experiment

sensor	Count of sensor error for target #5ID	Count of sensor error during target #2ID
1	0	0
2	0	0
3	0	0
4	0	0
5	2	3
6	0	0
7	0	0
8	0	0
9	1	1

Table 4.25 Count of sensor error during target localization experiment

Sensor	Count of sensor error for target #5LO	Count of sensor error for target #2LO
1	0	0
2	4	1
3	7	1
4	0	4
5	11	7
6	0	0
7	0	10
8	2	6
9	1	2

According to the experiences which we obtained during the tests, a good result for ILS system in continuous movement can be achieved if following items considered:

1. Use accurate and well operated sensors
2. Prepared a clean room (FREE of magnetic effects of other devices) for creating a dictionary.
3. Use big targets like a car
4. Discretizing the sensing region of the target to 4 sub-region (Figure.4.11.b)
5. Use different targets in terms of magnetic effect on sensor.

4.12.2 Sequential Localizing a Target on Continuous Movement

The main goal of the ILS system is identifying a target and online movement path exhibition. The results of previous section were used for setting up a reliable and accurate live ILS system in this section. The sensing region of the sensors was discretized to four sub-regions (Figure.4.11.b). Three of the best sensors were selected. The "mode method" which expressed in 4.12.1 was applied. MED method had the duty of the identification and localization decisions. A MATLAB code which combined with MED algorithm displays the estimated path.

During the experiments of this section we found that if two checking approach algorithm added to the decision part of ILS system, we will have more comprehensive estimation. These two checkers are "Threshold checker" and "Counter checker".

- **Threshold checker:** The first one is a threshold checker. For detecting a target, the magnetic intensity B_T (B_{TX} and B_{TY}) is comparing continuously with ambient value B_A (B_{AX} and B_{AY}) which is recorded at startup of the ILS system. From theoretical point of view, if absolute value of difference of B_T and B_A ($| B_T - B_A |$) is grater that zero, it means that there is a target(s) in the sensor sensing region. In practical, this principle

cannot be acceptable for all conditions. Suppose there is no defined target at sensor sensing region but there is random environment magnetic noise. This magnetic noise can be detected by magnetic sensors, so B_T will not equal to B_A. For reducing the noise affect, a threshold checker was added to main decision code. Threshold checker is adjustable by considering the entries of the Identification and localization dictionaries and the noise level. If the level of the noise is high, threshold level should be so near (or equal) to minimum entry of the identification and localization dictionaries. If the ILS system is operated in noiseless environment and sensors functioning well, the threshold checker can be selected so near (or equal) to zero. By trial and error during the experiments it is found that the ILS system cannot operate reliable without a proper threshold checker. The main disadvantage of threshold checker is reducing the sensitivity of the system.

- **Counter checker:** During the experiments observed that some times the level of the noise is more than the threshold checker level or sensors sending fake data and have incorrect measurements. These factors were affecting the tracking estimation incredibly. For eliminating these undesirable items, a counter checker was added to main decision code also. The counter checker operates as a buffer. It counts the number of the same decision which comes from estimator part the MED code. When this counter reaches to define value (count), it will announce the decision of the system to the plotter part of the code. By considering this decision the place and path of target will be display. After displaying, the counter value becomes zero and plotter goes to standby mode again. The counter checker is adjustable also. To define a "decision announcement value" (count) for counter checker, the number of the noise in the target movement interval from one cell to other cell, speed of the movement target and measurement accuracy of the sensor must be considered. If the number of the noise or the number of the error measurements of the sensors is high, large value must be selected for the "decision announcement value". For noiseless places when sensors function well or the movement speed of the target is high, this value must be selected as small as possible in order to have minimum delay in representation of the path. Delay in representing the location and path of the movement is the main disadvantage of the counter checker, but improvement of the estimation, by aid of it, is not undeniable.

The block diagram (Flowchart) of the ILS system with checker blocks is shown in Figure 4.12.o. As mentioned before, for this test the sensing region of each sensor is discretized to four cells. Required dictionaries were created by considering the section 4.9.1 explanations for four cells discretization. The real path and estimated path for different experiments are shown in following Figures.

Real path	Estimated path
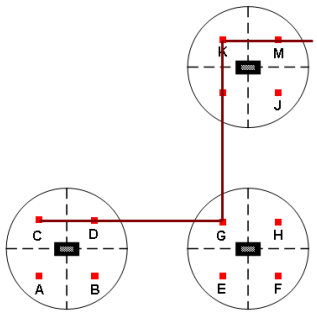	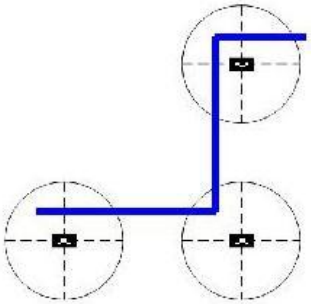
Entrance point : M Path : M➔K➔I➔G➔D➔C	Entrance point : M Path : M➔K➔I➔G➔D➔C

Figure 4.13.a Path number 1 (real path and estimated path)

Real path	Estimated path
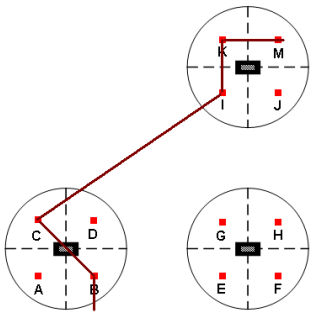	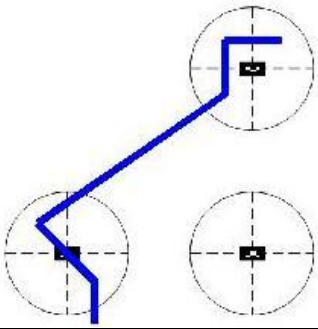
Entrance point : B Path : B➔C➔I➔K➔M	Entrance point : B Path : B➔C➔I➔K➔M

Figure 4.13.b Path number 2 (real path and estimated path)

Real path	Estimated path
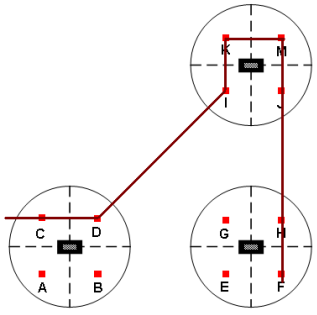	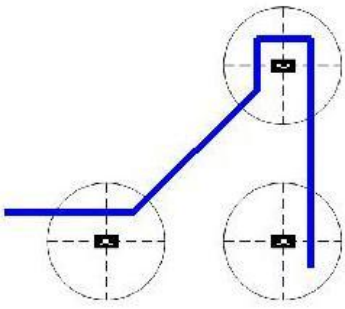
Entrance point : C Path : C➔D➔I➔K➔M➔J➔H➔F	Entrance point : C Path : C➔D➔I➔K➔M➔J➔H➔F

Figure 4.13.c Path number 3 (real path and estimated path)

Real path	Estimated path
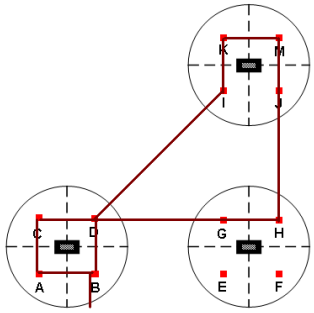	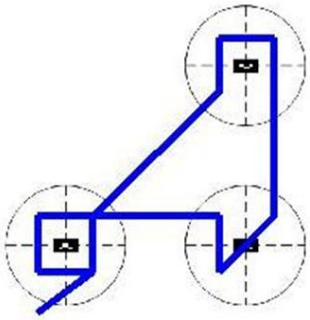
Entrance point : B Path:B➔A➔C➔D➔G➔H➔M➔K➔I➔D➔B	Entrance point : C Path:B➔A➔C➔D➔G➔E➔H➔M➔K➔I➔D➔B

Figure 4.13.d Path number 4 (real path and estimated path)

Real path	Estimated path
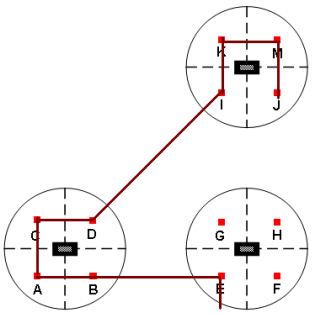	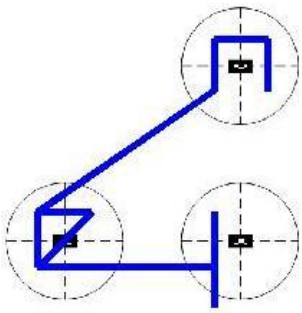
Entrance point : E Path : E➔B➔A➔C➔D➔I➔K➔M➔J	Entrance point : E Path : E➔G➔E➔B➔C➔D➔A➔C➔I➔K➔M➔J

Figure 4.13.e Path number 5 (real path and estimated path)

Real path	Estimated path
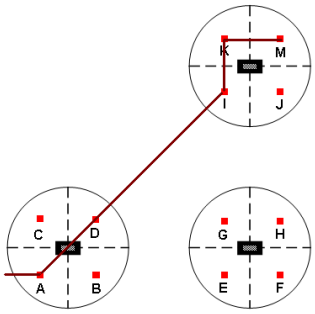	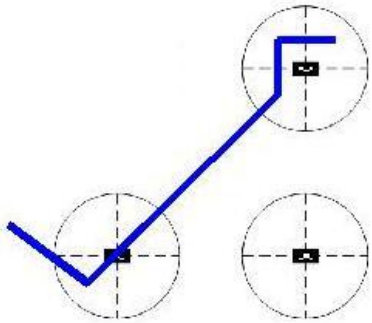
Entrance point : A Path : A➔D➔I➔K➔M	Entrance point : A (outer point estimated wrong) Path : A➔D➔I➔K➔M

Figure 4.13.f Path number 6 (real path and estimated path)

Real path	Estimated path
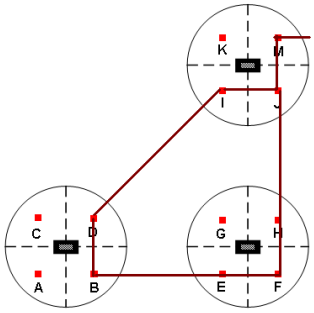	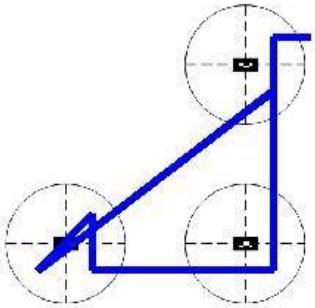
Entrance point : M Path : M➔J➔I➔D➔B➔E➔F➔H➔J	Entrance point : M Path : M➔J➔I➔A➔D➔B➔E➔F➔H➔J

Figure 4.13.g Path number 7 (real path and estimated path)

Real path	Estimated path
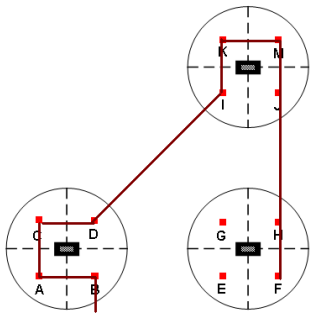	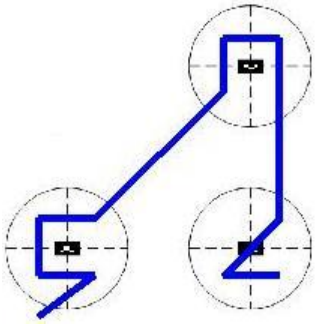
Entrance point : B Path : B➔A➔C➔D➔I➔K➔M➔J➔H➔F	Entrance point : B (outer point estimated wrong) Path: B➔A➔C➔D➔I➔K➔M➔J➔H➔E ➔F

Figure 4.13.h Path number 8 (real path and estimated path)

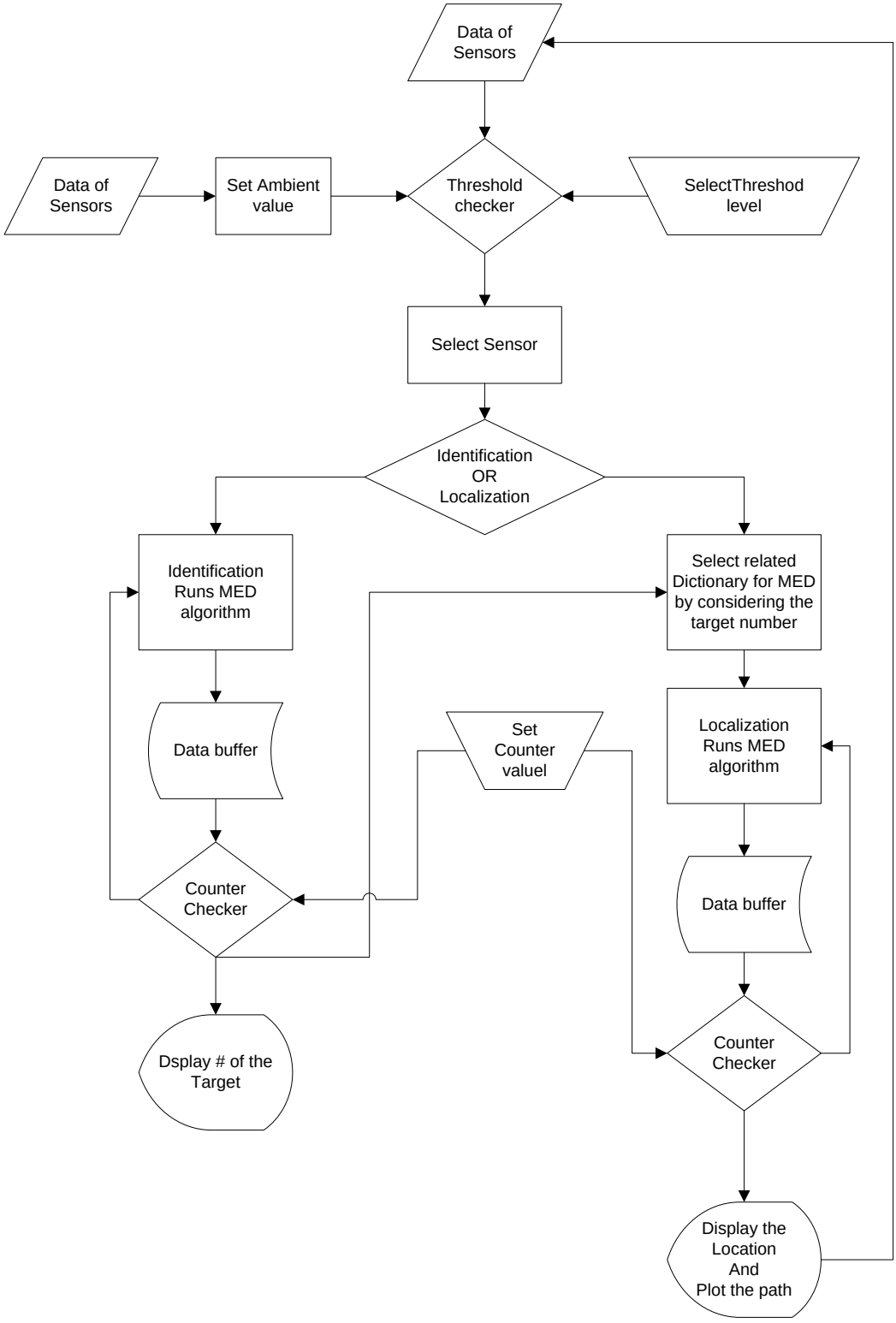

Figure 4.14 The block diagram (Flowchart) of the ILS system with checker blocks

CHAPTER 5

CONCLUSION & FUTURE WORK

By using Minimum Euclidean Distance (MED) method and a suitable dictionary, target identification and location estimation of the target are more possible. According to the observations during the test we found that if the magnetic characteristics of the targets are separable, the results of the experiments are reliable and accurate.

If we need to reduce the probability of error for target location estimation, the sensor coverage area should be divided into smaller cells. Number of the cells in the sensing region of a sensor defines the resolution of the ILS system for target localization process. By selecting large targets such as cars according to our experiments more accurate results can be obtained. In future works different types of cars can be considered as test targets for identification and localization.

Since HMC1002 magnetometers are sensitive to temperature changes, so the temperature of the environment should be fixed at a specific degree while creating a dictionary for MED and also during the localization and identification tests. Another solution to deal with temperature effect is to update the ambient value when any temperature changes are observed. Using isolation boxes for nodes to fix the temperature of the environment of the nodes and editing the software part of the ILS system (updating ambient value by observing any temperature changes) could be proposed as other jobs for next step of the research.

In the course of an experiment the power supply level should be under control. According to the results of section 4.6 the measured value changes when power supply level changes. Adding an ambient updater block to the software of the ILS system could be a software solution for eliminating the effect of the power supply level changes. This block checks the power supply level. If any power variation is detected, it will update the ambient value to a new value. To cope with power supply level variation issue, controling the power level and charging the power source continually is a practical solution. For this purpose adding energy harvesting circuits to the mots is one of our future works. Different kinds of harvesters such as solar, piezoelectric and wind will be used. Providing the energy of the sensors in remote control form by RF technology is in our list for future works. For a network with limited energy for sensors, optimizing the function of the sensors is critical work. This optimization contains design a customized protocol

for the network, modifying the activation time of the sensors and organizing sleep mode for the sensor properly. These solutions are considered for next challenges of our research team.

AMR sensors sense any magnetic change. Unpredictable magnetic noises can destroy the target magnetic field. Creating required dictionaries and doing the experiments in a clean room (Free magnetic place) is a good idea. For practical cases having a clean room is not possible. Adding a threshold checker before decision block of the algorithm is an effective approach.

Well functioning sensors have important role for ILS systm. Checking the sensors before an experiment can increase the accuracy of the estimation. During the experiments sometimes the sensors distribute the fake data. A data buffer and a counter after MED estimator and before the path plotter can omit these wrong data.

Identification and Localization is done on the PC side via the Minimum Euclidean Distance (MED) Method. For different localization cases different results were obtained. In specific case when sensing region was discretized to four sub-region (section 4.11.3) location estimation of a target in the performance of the MED method was 100% under fixed temperature, no magnetic noise and fixed voltage power level. This case was used in continuous movement test and the performance of the WSN is investigated for sequential localization.

There is random delay in the network operation and illustration part of the ILS system due to processing delay caused by TinyOS, the threshold checker and counter checker, random back-off in the MAC layer, transmission of reliable magnetic readings to PC via the physical layer, and delay caused by MED method, but overall according to the test results these delays are still negligible for slow movement. For high speed movements the software, hardware and algorithm must be readjusted with new conditions. Considering these items could be another task for future work.

Results of the section 4.10 show that if target entrance point is not known to MED method the performance of the ILS system for identification is not acceptable. For known entrance point cases there are some errors. By identifying the target when a target enter to and leave the sensing region of a sensor the identification performance can be increase.

In future work, we intend to investigate tracking and energy efficiency concepts. Kalman filter based methods, particle filtering and iFilter could be used for tracking a target. Customized protocol for the network could increase the performance and life time of the network. Designing a new protocol for the network is in the list of the future work of the METU CNG research team.

In this study single target single sensor (STSS) case is considered. For generating a sparse network sensors were distributed in the test region such that there is no intersection in their sensing regions. By considering this condition at any time a target is at sensing region of a sensor. If the numbers of the targets are more than one it means multi-target (MT) or the sensors cover their adjacent sensors sensing region (MS) a new method should be applied in ILS system. The MED is a degenerate version of an iterative greedy algorithm which is called Orthogonal

matching pursuit (OMP). OMP could be one of the good solutions for multi-target and non-sparse WSN for target identification, localization, and tracing.

An iterative greedy algorithm which may be used in our ILS system is the Orthogonal Matching Pursuit (OMP) [29] algorithm. OMP is a sparse approximation technique, such as "basis pursuit" [30] and "matching pursuit" [31]. OMP tries to find the "best matching" projections of multidimensional data onto an over-complete dictionary D with a predefined number of iterations. In each iteration, the column of dictionary "D" having maximum correlation with that iteration's residual "r" is selected. This locally optimum solution is recorded as i^{th} element of the coefficient vector "C" where the "i" shows the step (iteration) number. This algorithm is modified version of an earlier algorithm called Matching Pursuit (MP).

In order to use Orthogonal Matching Pursuit (OMP) algorithm we need a dictionary which is created by using signal parametric model. In our testbed we can divide the sensing region of each sensor to 28 sub-regions and 4 sub-regions and obtain data from each point for generating a dictionary. Each element of the dictionary "D" is named atom. These operations are so similar to steps of MED method. The tested signal can be recovered by combination of correct items (χ) in minimum iteration. That is why the title "iteration" is attributed to this algorithm:

$$\hat{\mathbf{s}} = \sum_{j=1}^{J} C_j \cdot \hat{\boldsymbol{\chi}}\left(\xi_\eta\right) \tag{5.1}$$

where :

- η is the index of the items in the dictionary D
- ξ is the parametric vector of the model
- J is the number of the items required for recovering the test signal
  since this is a sparse approximation J<<Q (total number of the items)
- C_j is the j^{th} element of the coefficient vector C

And the coefficient vector "C" is generated as follows:

1. Set the index to zero (η=0)
2. Set residual signal (r) equal to the tested signal. ($r_0=\chi$)
3. Set the loop index (t) equal 1 (t=1).
4. Determine the dictionary item having the largest orthogonal projection on the residual signal (r).
5. Calculate the following MSE

$$\min\left\|\chi - \sum_{j=1}^{t} C(\eta_j)\hat{\chi}(\eta_j)\right\|_2 \tag{5.2}$$

6. Update the residual signal by substracting the signal components found in step 5.

$$\mathbf{r_t} \Rightarrow \chi - \sum_{j=1}^{t} C(\eta_j)\hat{\chi}(\eta_j) \tag{5.3}$$

7. Increment the loop index (t=t+1)
8. If stopping criteria not satisfied go to step 2 else finished.

For OMP algorithm there exists varies kind of stopping criteria for example: error rates falls below a specific value, presence of a specific target and like these. Since in practical cases we can not limited the number of the targets on the monitoring area, so multi-target (MT) cases applying OMP on ILS system should be considered as another task for future work.
OMP algorithm is also illustrated below in pseudocode.

OMP Algorithm:

Input:

- A d-dimensional target signal s and matrix D.
- Stopping criterion e.g. until a level of accuracy is reached

Output:

- A coefficient vector c

1.	$\Lambda_0 = \emptyset$	{ Initialize the index set }
2.	$r_0 \leftarrow s$	{ Residual }
3.	**for** t=1 to I **do**	{ I=Dimension of the Dictionary D}
4.	$\lambda_t \in \arg\max_w \lvert < r_{t-1}, \varphi_\omega > \rvert$	{ Selection}
5.	$\Lambda_t \leftarrow \Lambda_{t-1} \cup \{\lambda_t\}$	{ Update the index set}
6.	$\min_{c \in c^{\Lambda_t}} \lvert\lvert s - \sum_{j=1}^{t} c(\lambda_j)\varphi_{\lambda_j} \rvert\rvert_2$	{ Solution c of the least-squares problem }
7.	$r_t \leftarrow s - \sum_{j=1}^{t} c(\lambda_j)\varphi_{\lambda_j}$	{New residual by using coefficients c }
	end for	
8.	return c	{maximum of c}

REFERENCES

[1] Dhar, A.; Kulkarni, P.; “Using magnetic sensors to estimate street traffic patterns” www.cse.iitb.ac.in. (Last visited on May 2012)

[2] Cheung, S.Y.; Coleri, S.; Dundar, B.; Ganesh, S.; Tan, C.; Varaiya, P.; “Traffic Measurment and Vehicle Classification with a Single Magnetic Sensor,” UC Berkeley, PATH paper, 2004.

[3] Lee, S.; Yoon, D.; Ghosh, A.; “Intelligent parking lot application using wireless sensor networks,” Int. Symp. on Collaborative Technologies and Systems (CTS), 19-23 May 2008, sf. 48-57.

[4] Boda, V.K.; Nasipuri, A.; Howitt, I.; “Design consideration for a wireless sensor network for locating parking spaces,” in Proc. SoutheastCon, 2007.

[5] Cheung, S.Y.; Ergen, S.C.; Varaiya, P.; “Traffic surveillance with wireless magnetic sensors,” U.C. Berkeley, California PATH Research Report, 2007.

[6] Kaewkamnerd, S.; Chinrungrueng, J.; Pongthornseri, R.; Songphon Dumnin; "Vehicle classification based on magnetic sensor signal," Int. Conf. on Inf. and Automation (ICIA), 20-23 June 2010, sf.935-939.

[7] Dimitropoulos, K.; et. al.; “Detection, tracking and classification of vehicles and aircraft based on magnetic sensing technology,” Trans. Eng. Computing and Tech., Vol. 14, 2006, sf. 161-166.

[8] Antepli, M.A.; Gurbuz, S.Z.; Uysal-Biyikoglu, E.; “Ferromagnetic target detection and localization with a wireless sensor network,” MILCOM 2010

[9] Wikipedia. Simulated annealing. http://en.wikipedia.org/wiki/Simulated_annealing. (Last visited on May 2012)

[10] Tropp, J.A.; Gilbert, A.C.; "Signal recovery from random measurements via orthogonal matching pursuit," Trans. Info. Theory, Vol.53, No.12, Aralık 2007, sf. 4655-4666.

[11] Cai, T.T.; Wang, L.; “Orthogonal matching pursuit for sparse signal recovery with noise,” Trans. Information Theory, Vol.57, No.7, Temmuz 2011, sf. 4680-4688.

[12] Gürbüz, S.Z.; Melvin, W.L.; Williams, D.B.; “Radar-based human detection via orthogonal matching pursuit,” ICASSP, 2010.

[13] Gurbuz, A.C.; Scott, W.R.; McClellan, J.H.; "Location estimation using a broadband electromagnetic induction array", Proc. SPIE, Vol. 7303, 2009.

[14] MPR-MIB Users Manual- Revision A, June 2007 - PN: 7430-0021-08.

[15] Sensor Network Motes: Portability & Performance , Ph.D. dissertation by Martin Leopold.

[16] Chipcon AS SmartRF CC2420 Preliminary Datasheet (rev 1.2), 2004-06-09.

[17] MTS/MDA Sensor Board Users Manual, Revision A, June 2007, PN: 7430-0020-05.

[18] C. Johansson, C. Jonasson, and M. Erlandsson, “Magnetic Sensors for Trafic Detection,” Imego AB, 411 33 G¨oteborg, Sweden, Tech. Rep. 110078-rapport, 2006.

[19] P. Ciureanu, S. Middelhoek, “Thin Film Resistive Sensors”, 1992, NewYork: Institute of Physics Publishing.

[20] Michael J. Caruso, Lucky S. Withanawasam , “Vehicle Detection and Compass Applications using AMR Magnetic Sensors” , Honeywell SSEC 12001 State Highway 55, Plymouth, MN USA 55441 <www.ssec.honeywell.com>. (Last visited on May 2012)

[21] Vehicle Detection Using AMR Sensors, Application Note AN218, Honeywell International,Solid State Electronics Center. [Online]. Available: http://www.ssec.honeywell.com. (Last visited on May 2012)

[22] Honeywell Magnetic Sensors Product Data Sheet, “1- and 2-axis magnetic sensors,” Honeywell SSEC, 2004.

[23] ALPHALAB INC. Meters for Magnetism. http://www.trifield.com. (Last visited on May 2012)

[24] A. J. Verweerd, "Performance Analysis and Characterisation of a new MagnetoElectrical Measurement System for Electrical Conductivity Imaging", page 33.

[25] W. J. Broad, “Will Compasses Point South?” New York Times, July 2004. [Online], Available: http://www.nytimes.com. (Last visited on May 2012)

[26] Google. Google Earth. http://www.google.com. (Last visited on May 2012)

[27] Wikipedia. Magnetostatics. http://en.wikipedia.org/wiki/Magnetostatics. (Last visited on May 2012)

[28] Griffiths, D.J.; Introduction to Electrodynamics. Prentice Hall, 1999.

[29] Pati, Y.C.; Rezaiifar, Y.C.; Krishnaprasad, P.S.; “Orthogonal matching pursuit: recursive function approximation with applications to wavelet decomposition,” in Proc. 27th Asilomar Conf., 1993.

[30] Wikipedia. Basis pursuit. http://en.wikipedia.org/wiki/Basis_pursuit. (Last visited on May 2012)

[31] Wikipedia. Matching pursuit. http://en.wikipedia.org/wiki/Matching_pursuit. (Last visited on May 2012)

[32] Wikipedia. Kelvin. http://en.wikipedia.org/wiki/Kelvin. (Last visited on May 2012)